

Imaging of Plasma Flows and Current Density in Tokamaks

Ahmed Diallo

Princeton Plasma Physics Lab

In Collaboration with

J. Howard¹, M. Creese¹,

S. Allen², R. Ellis², W. Meyer², R. Jaspers³, J.Koning³,

J. Chung⁴, R. Boivin⁵, M. Van Zeeland⁵

¹ *Plasma Research Laboratory, Australian National University*

² *Lawrence Livermore National Lab, CA*

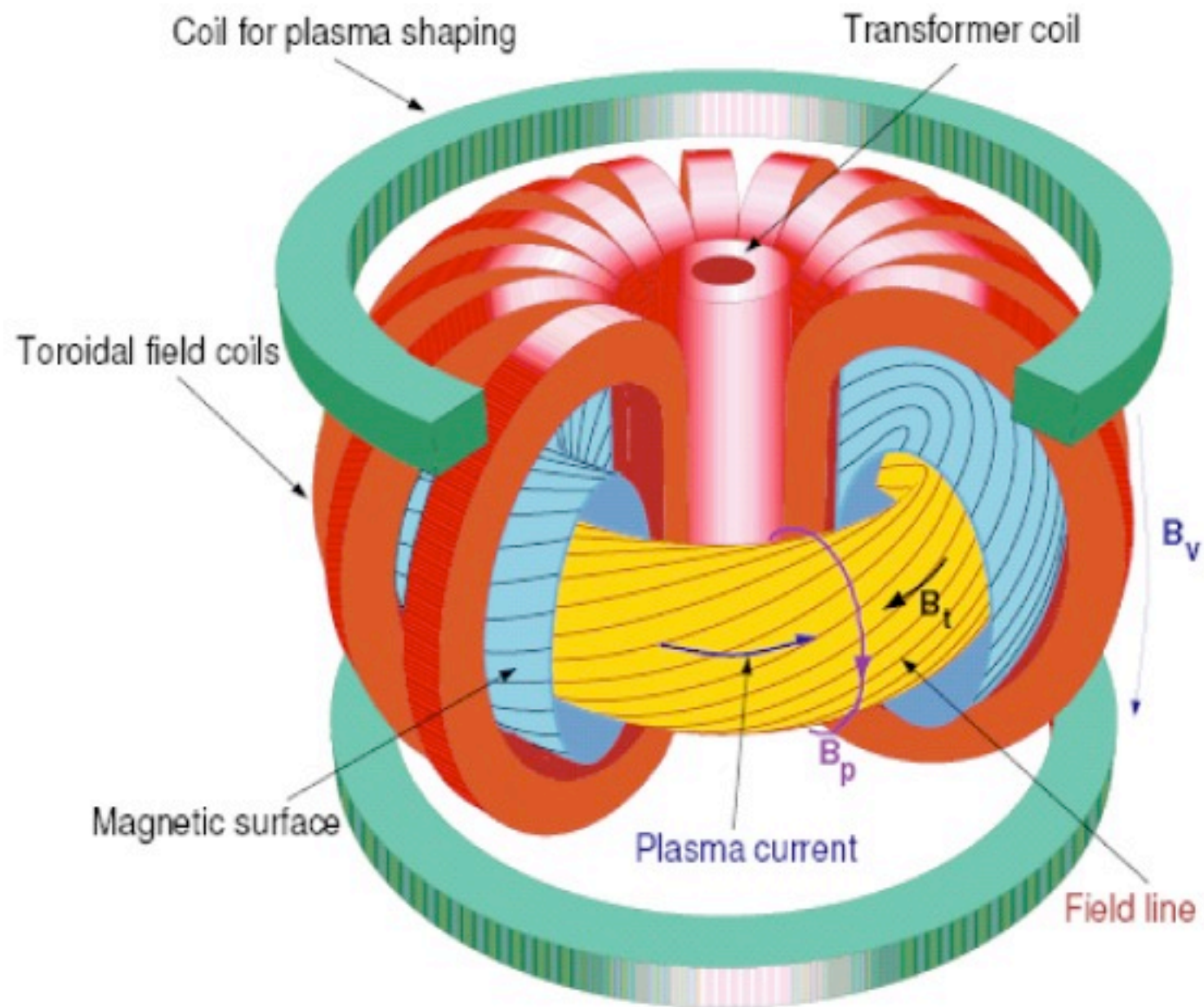
³ *FOM & TEXTOR, Germany*

⁴ *KSTAR, Korea*

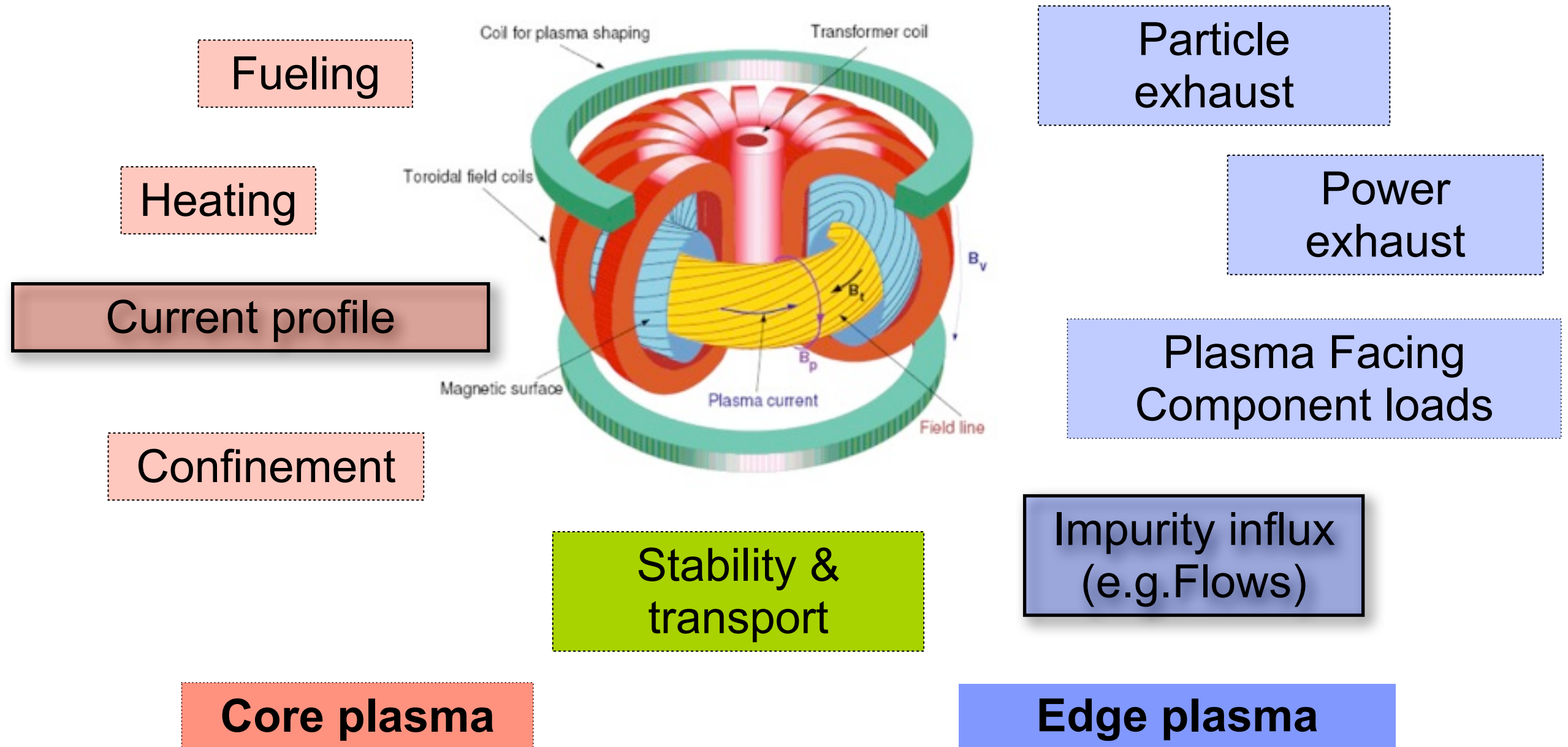
⁵ *General Atomics DIID, CA*

APS- April Meeting 2010 Washington DC -13/02/2010

Tokamak Schematic



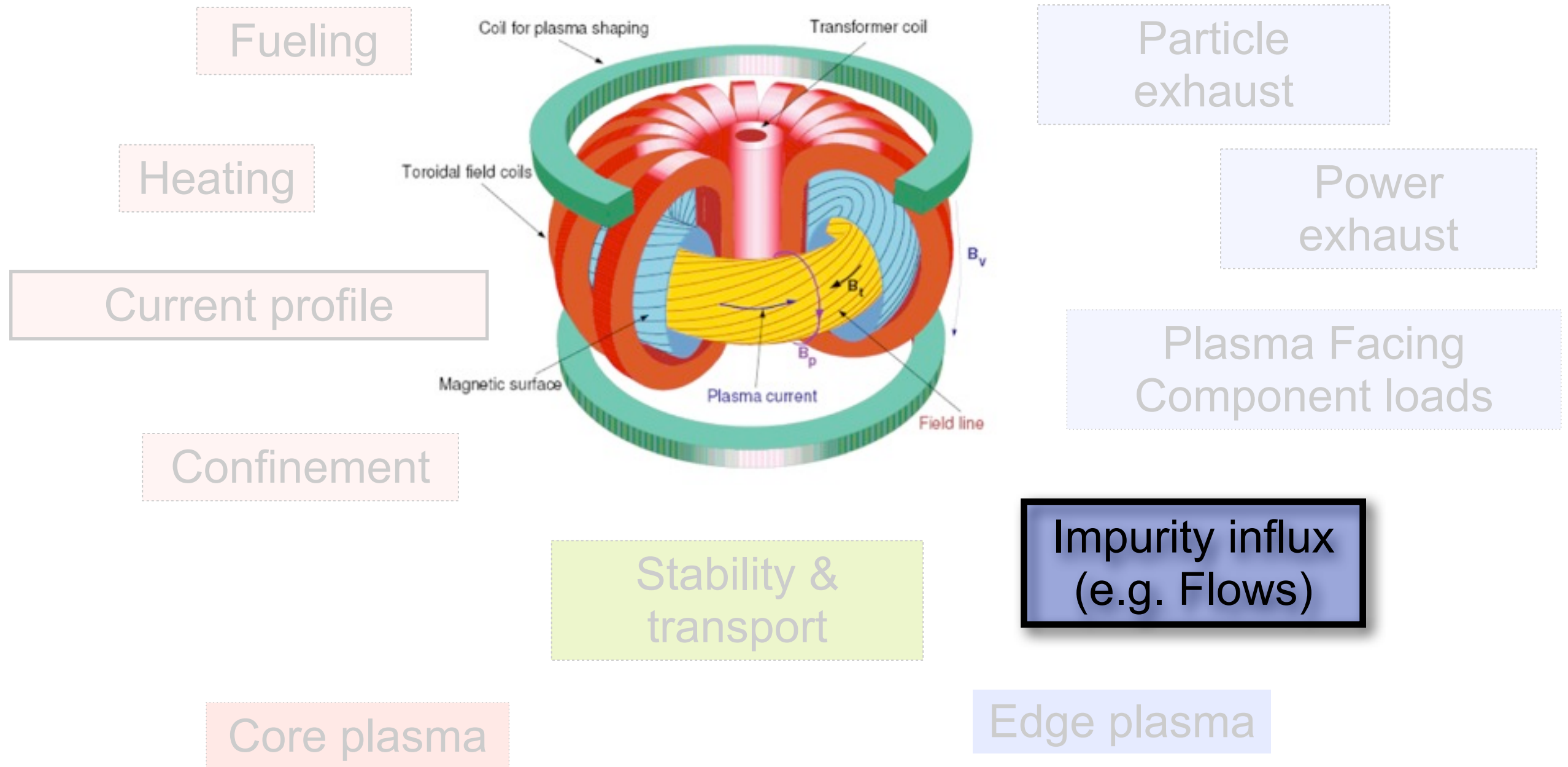
Key Components of Plasmas Generated in a Tokamak



Outline

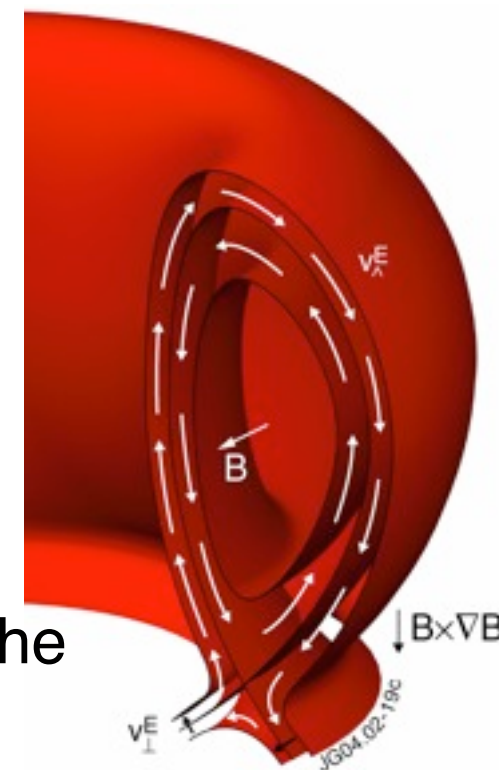
- How to image flows and the current profile?
 - Polarization interferometer
 - Spatial heterodyne system
- Applications
 - Doppler flow measurements (DIID)
 - Magnetic field pitch angle map (TEXTOR)
- Summary and Outlook

Key Components of Plasmas Generated in a Tokamak



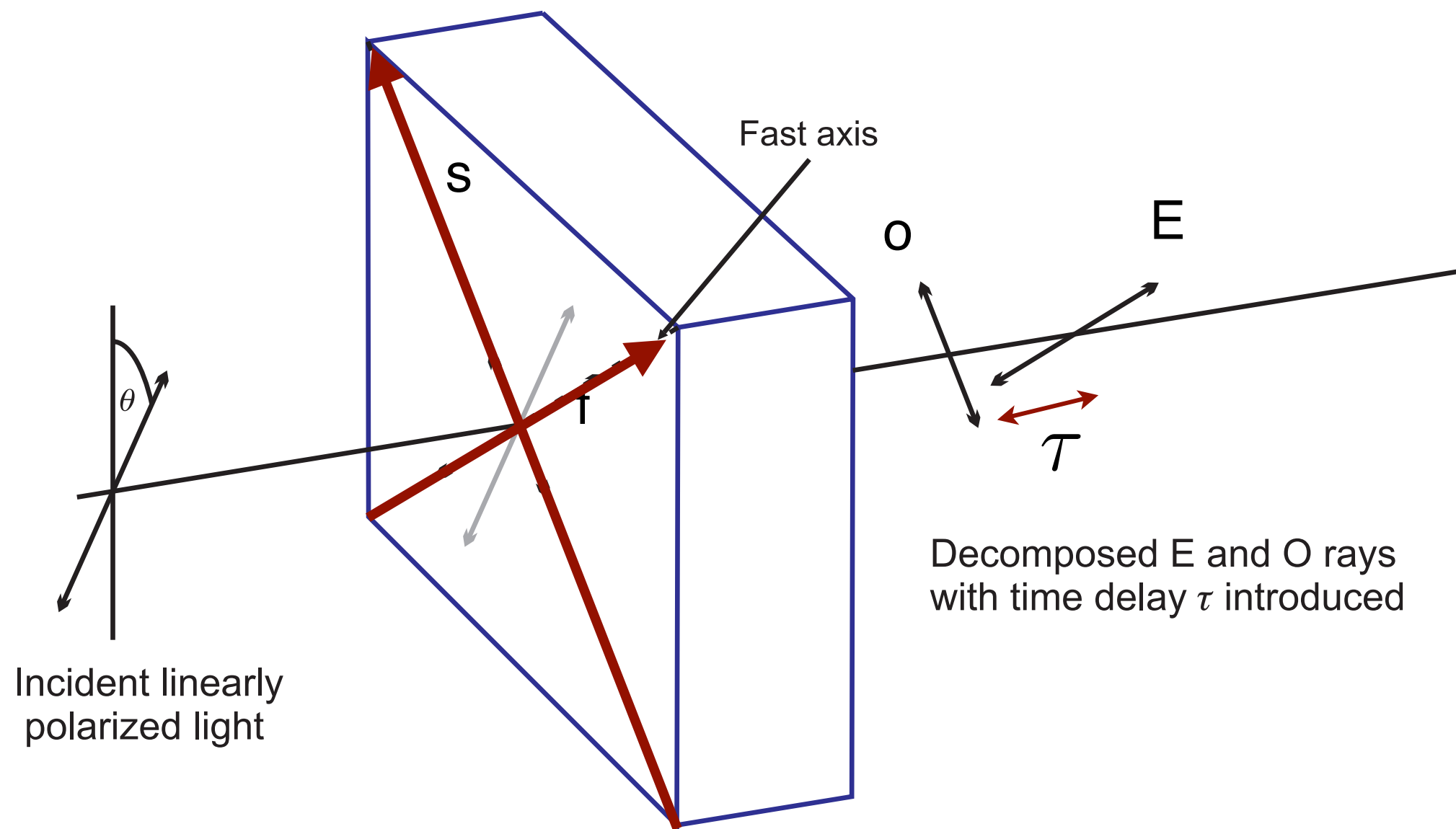
Hurricane-like Flows in the Edge of Tokamaks

- Edge used for material migration: balance of material and redeposition inner and outer divertor
- Current edge flow measurement diagnostics include
 - Doppler spectroscopy - single points - poor spatial resolution
 - Mach probe - Intrusive and of limited spatial reach in plasmas
- Flows are known to suppress turbulence: improves plasma performance
- Comparison coupling mechanism between the core plasma rotation and the edge flows.
- Experimental validation of arrays of edge modeling simulations required
- **A comprehensive picture of edge flows calls for an imaging technique**



Standard Waveplate: Overview

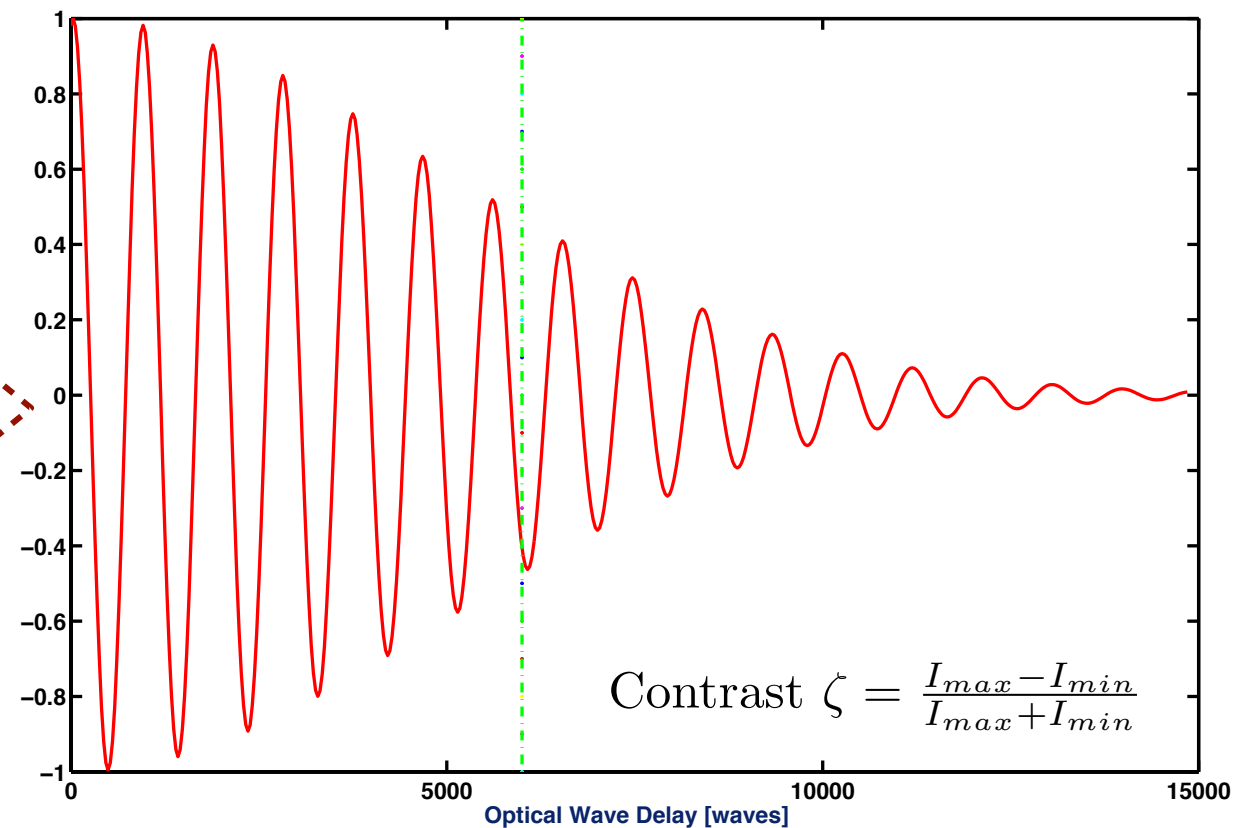
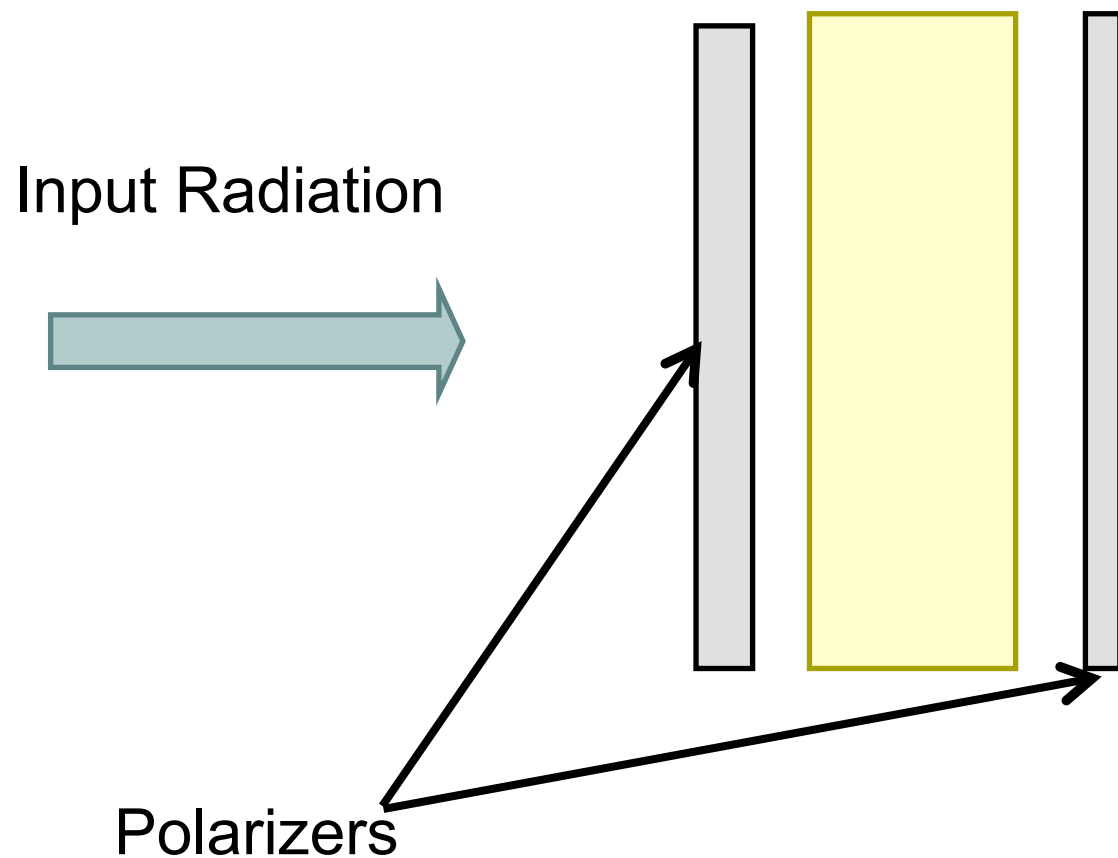
Optical axis in the plane of incidence



Recall a Simple Polarization Interferometer

Waveplate $\varphi = \frac{2\pi |n_e(\lambda) - n_o(\lambda)| L}{\lambda}$

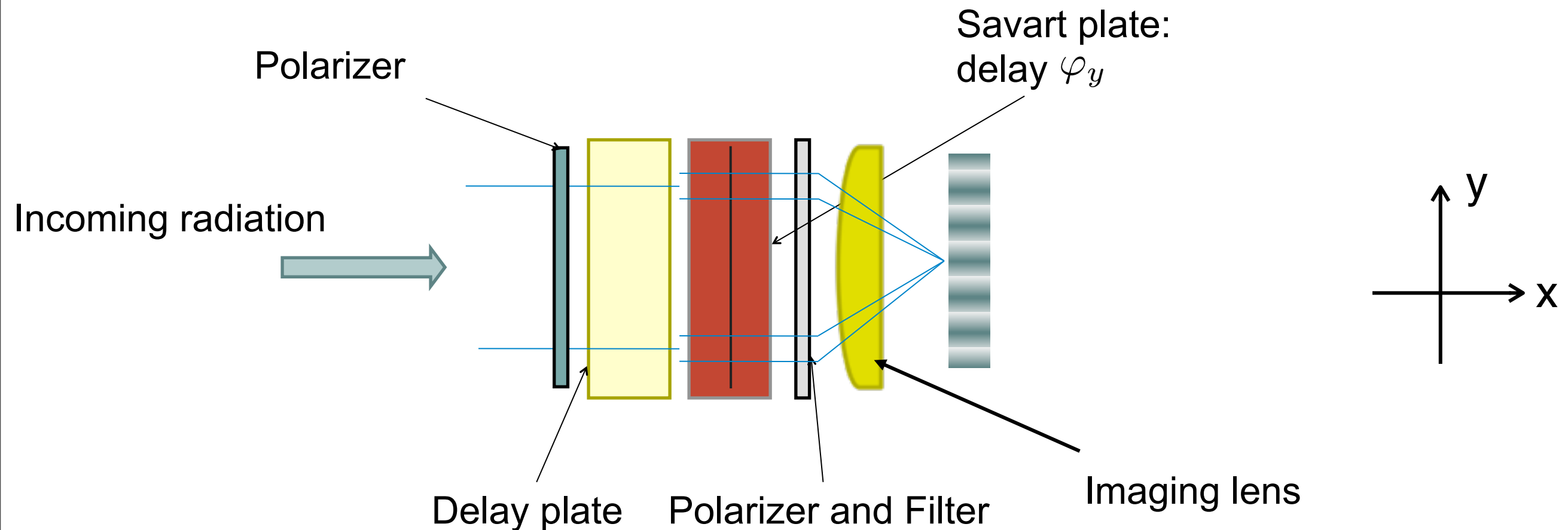
$$S = I(1 + \zeta \cos\varphi)$$



- These interferometers have higher throughput
- Allow for 2D spectral imaging
- Requires multiplexing independent images to extract the phase shift

Shearing Polarization Interferometer: Description

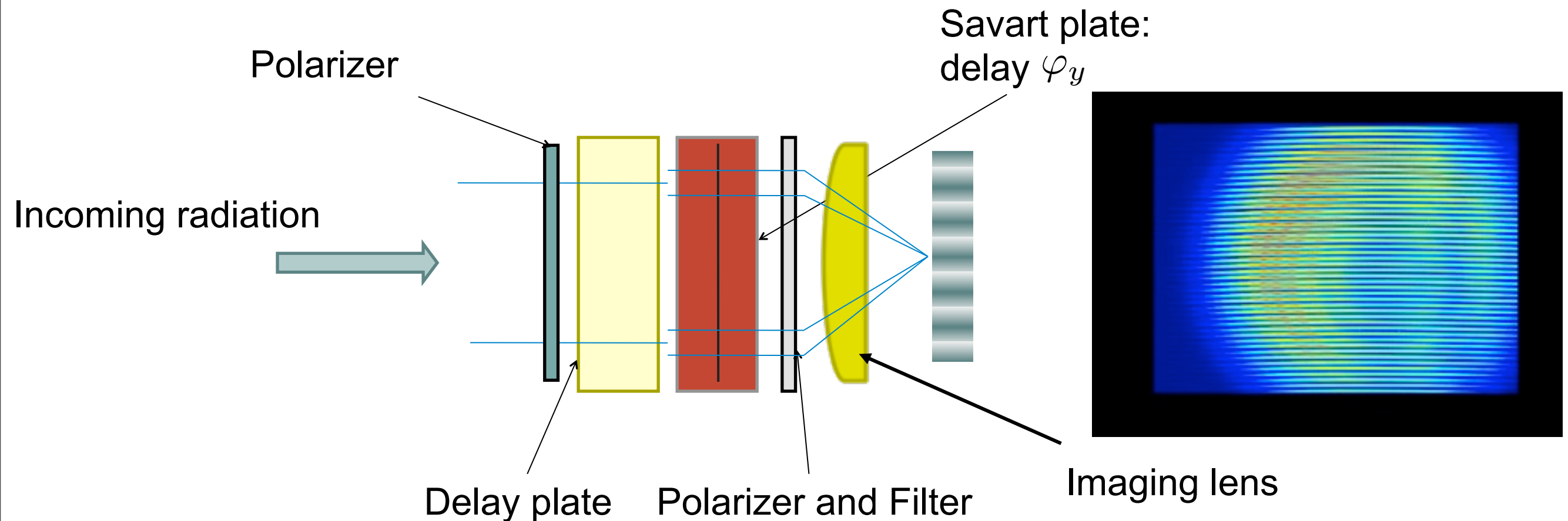
Insert shearing (Savart) waveplate:



$$S = I[1 + \zeta \cos(k_y y + \varphi)]$$

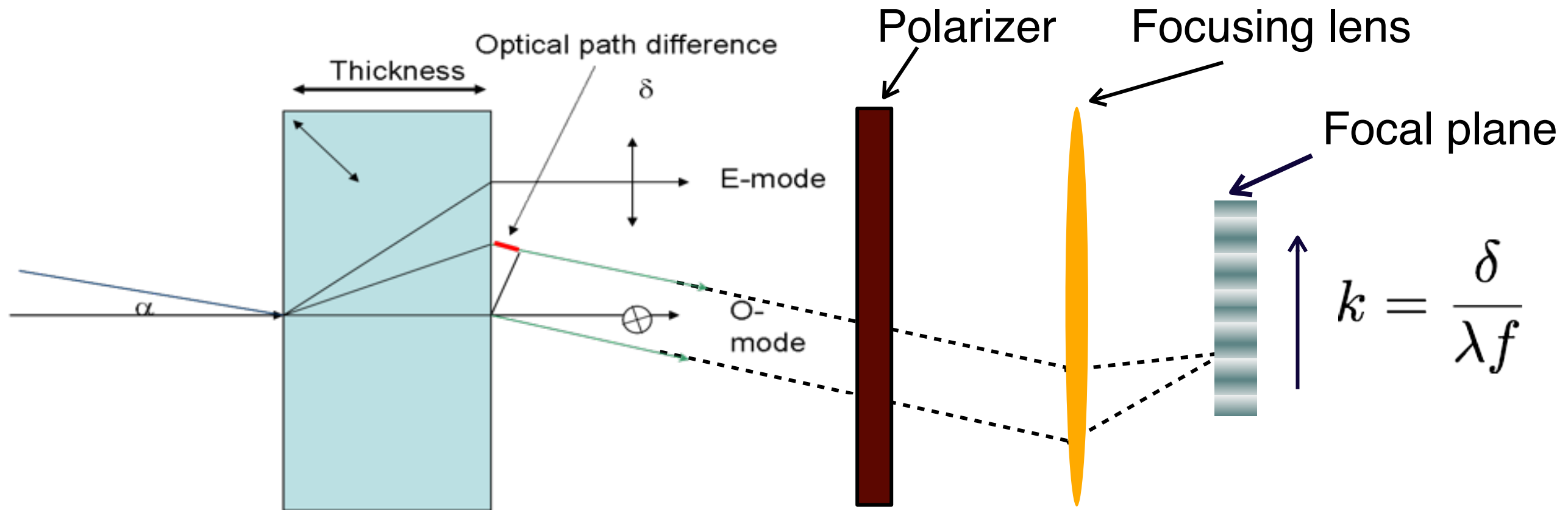
Shearing Polarization Interferometer: Description

Insert shearing (Savart) waveplate:



$$S = I[1 + \zeta \cos(k_y y + \varphi)]$$

Generation of Spatial Fringes using a Savart Plate



$$\delta = [A(n_e, n_o) + \frac{n_e^2 - n_o^2}{n_e^2 + n_o^2} \underbrace{\cos \eta}_{\sqrt{2}/2} \sin \alpha] \text{ Thickness}$$

The ray separation generates an angle-dependent path difference:
fringes enable spatial modulation

Interpreting the Interferogram

- The mean interferometer signal gives the line integrated brightness:

$$S_0 = \int I_0(r) dl$$

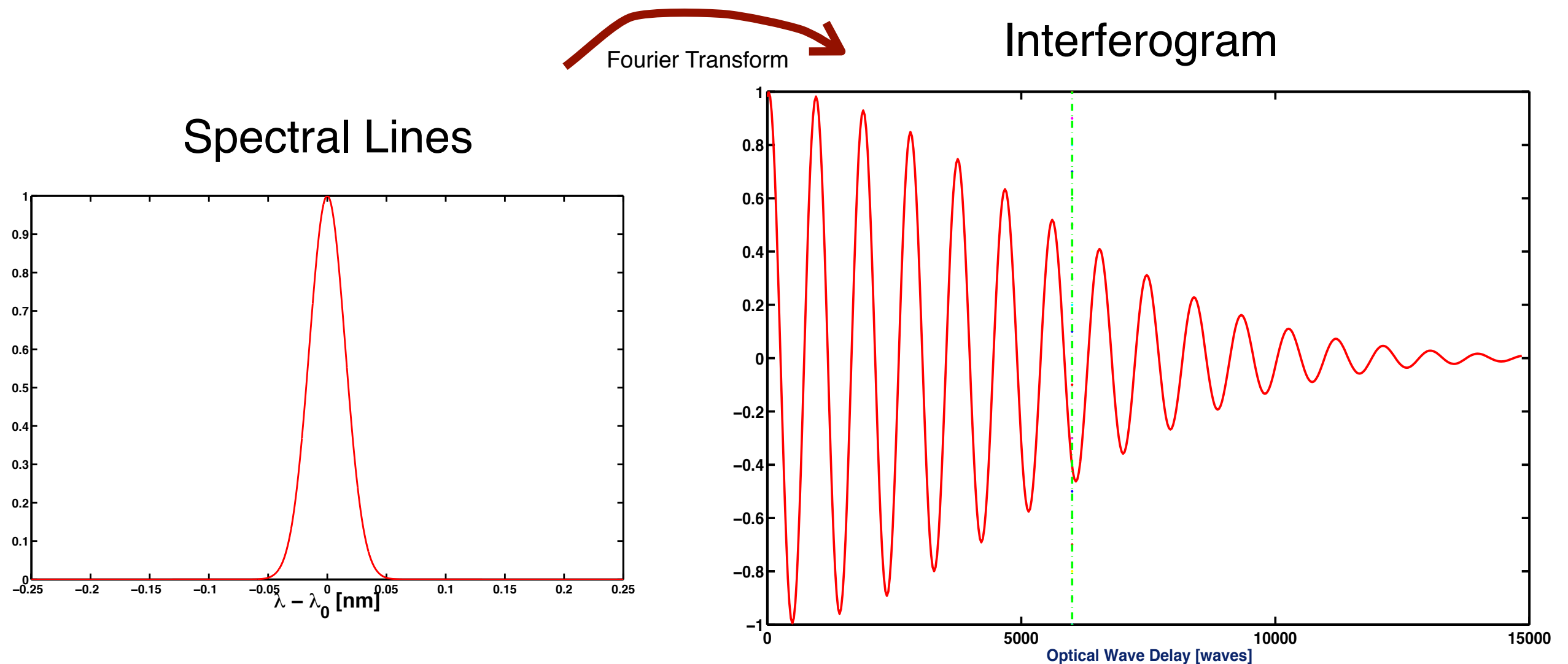
- The fringe visibility yields the temperature:

$$\langle \xi \rangle = \int I_0 \xi(r) dl \text{ where } \xi(r) = e^{-T(r)/T_{crystal}}$$

- The change in interferometer phase gives line integrated Doppler shift:

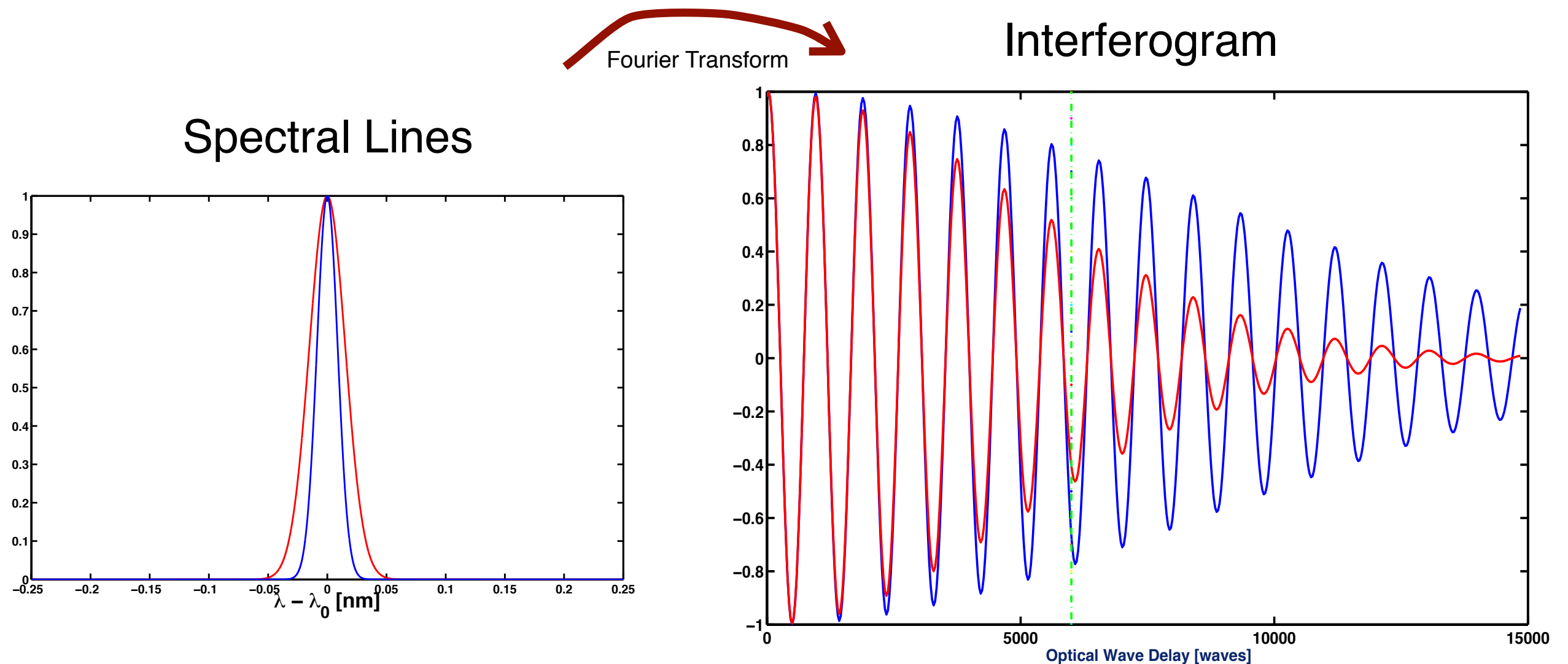
$$\frac{\delta\varphi}{\varphi} = \int I_0 \xi(r) \frac{\vec{v}_0}{c} \cdot \hat{l} dl$$

Temperature and Doppler shift of Spectral lines are Encoded on the Interferogram



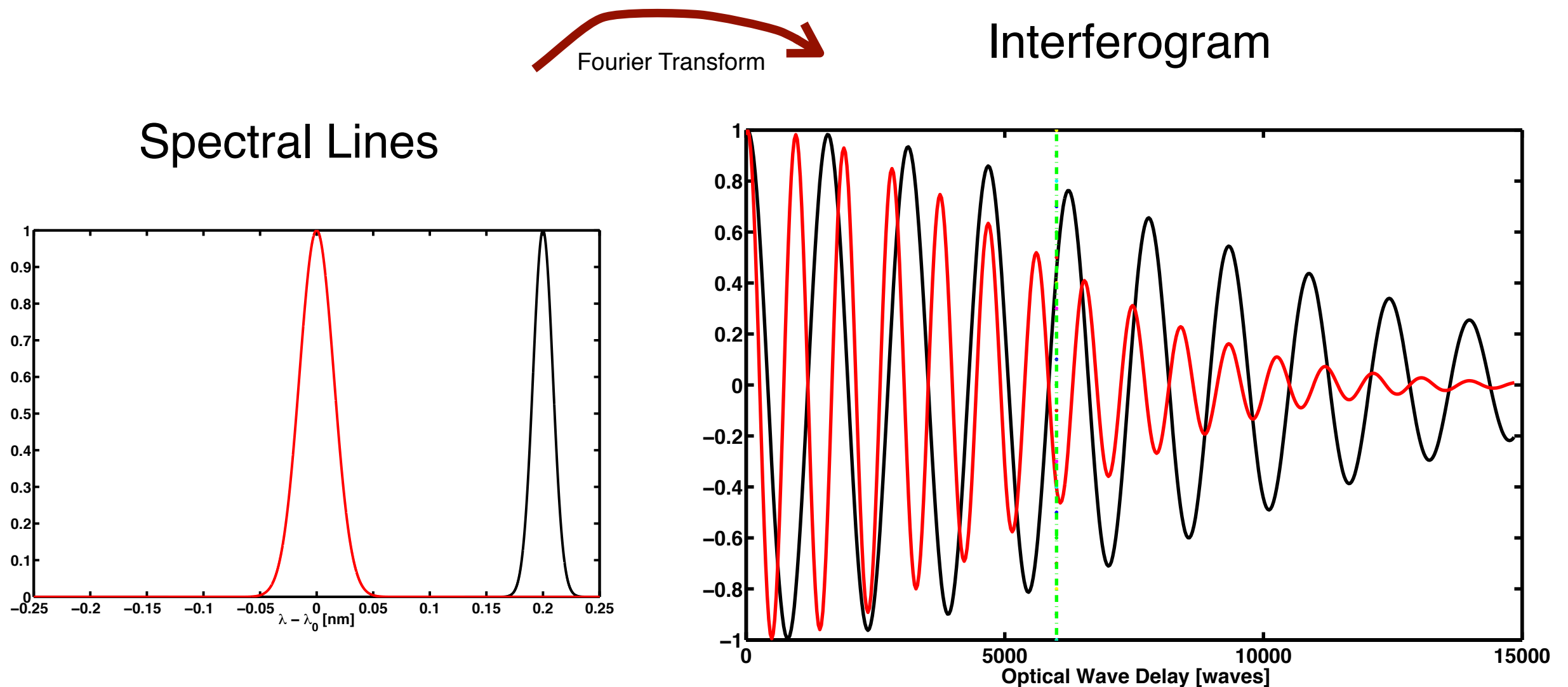
- The visibility tracks the line broadening (temperature)
- The relative phase shift is proportional to the line shift (flow)

Temperature and Doppler shift of Spectral lines are Encoded on the Interferogram



- The visibility tracks the line broadening (temperature)
- The relative phase shift is proportional to the line shift (flow)

Temperature and Doppler shift of Spectral lines are Encoded on the Interferogram



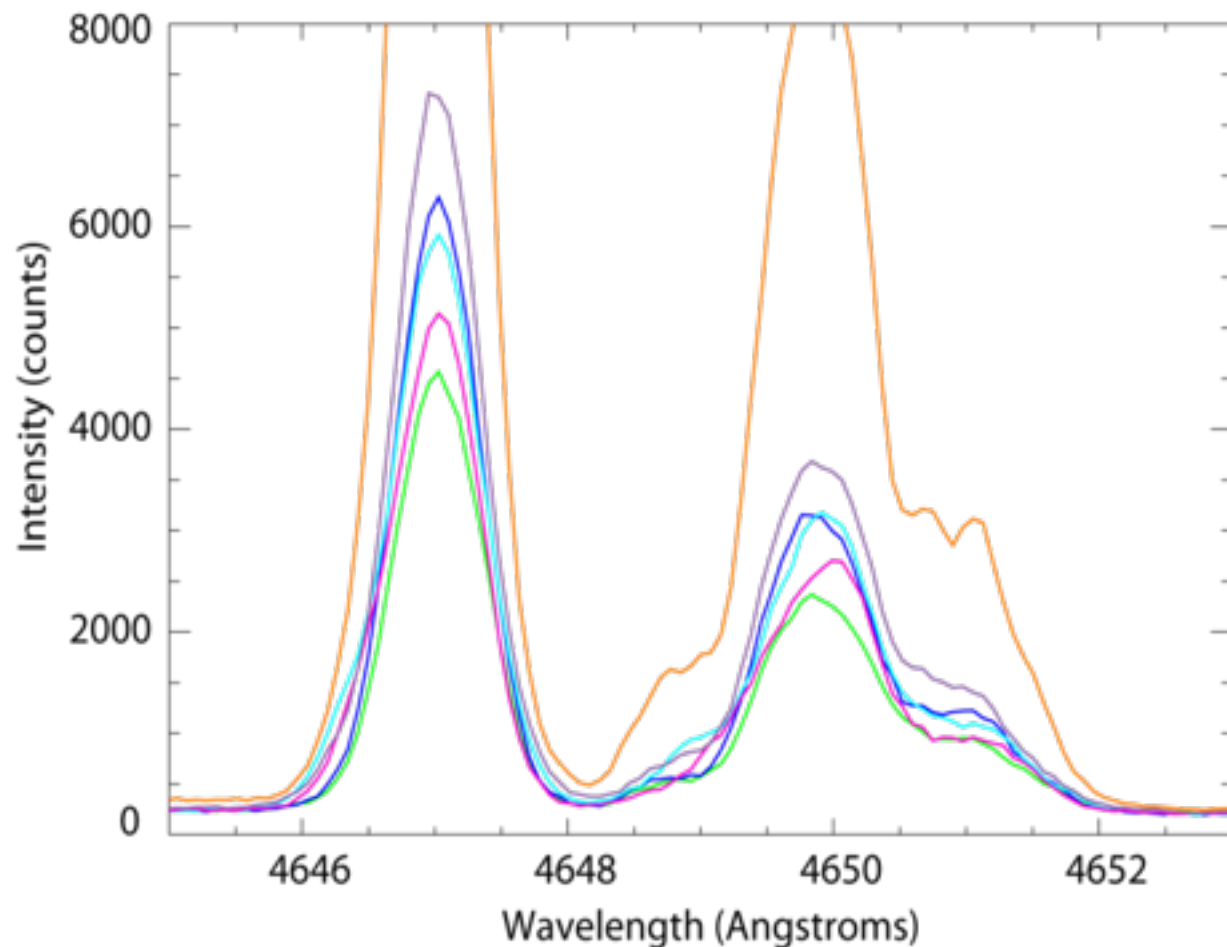
- The visibility tracks the line broadening (temperature)
- The relative phase shift is proportional to the line shift (flow)

Outline

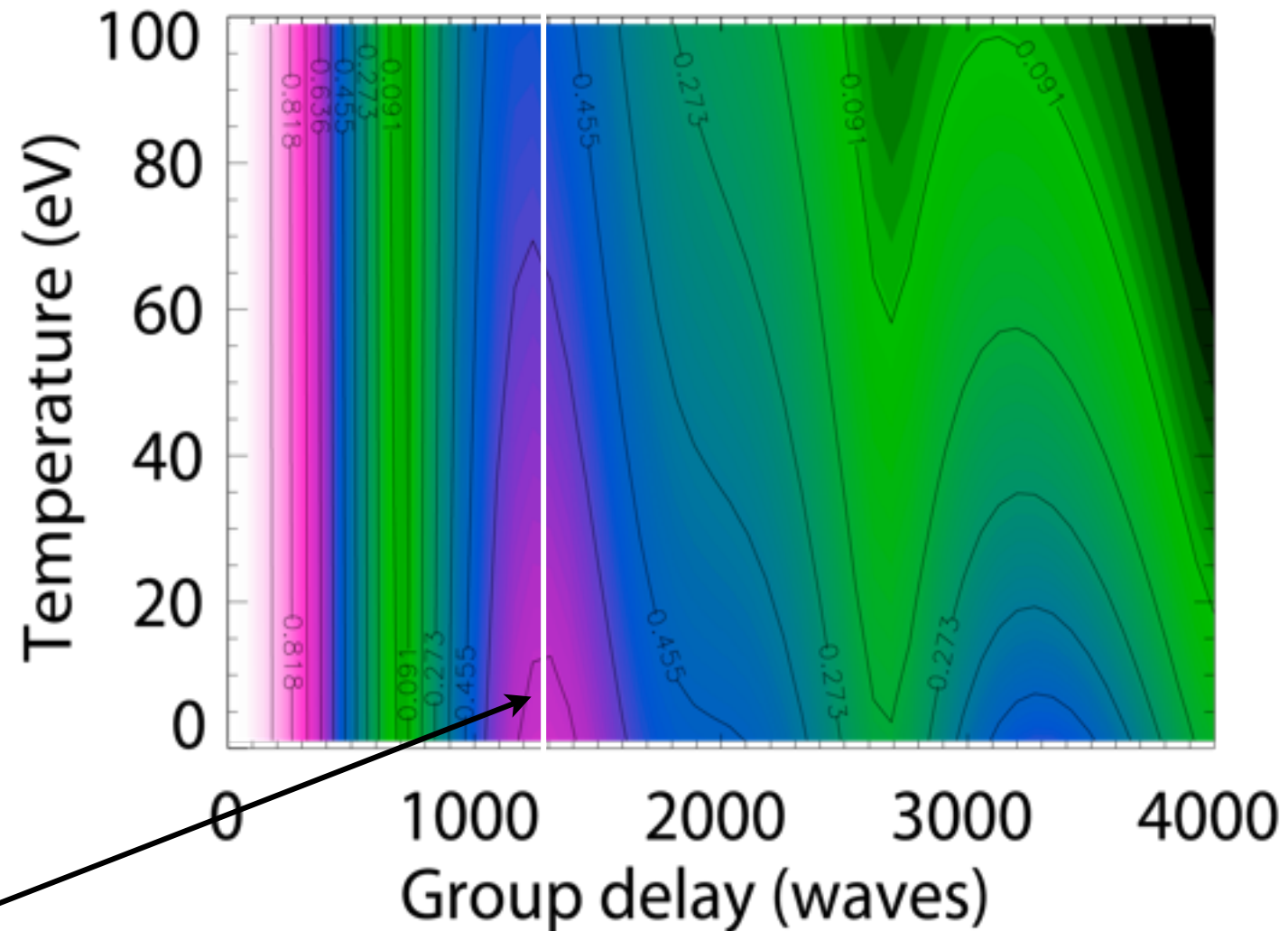
- How to image flows and the current profile?
 - Polarization interferometer
 - Spatial heterodyne system
- **Applications**
 - **Imaging of Doppler flows (DIIID)**
 - Magnetic field pitch angle map (TEXTOR)
- Summary and Outlook

Modeling CIV @ 465nm Optical Coherence: Fourier Transform of the Line Shape

Measured CIV Multiplet



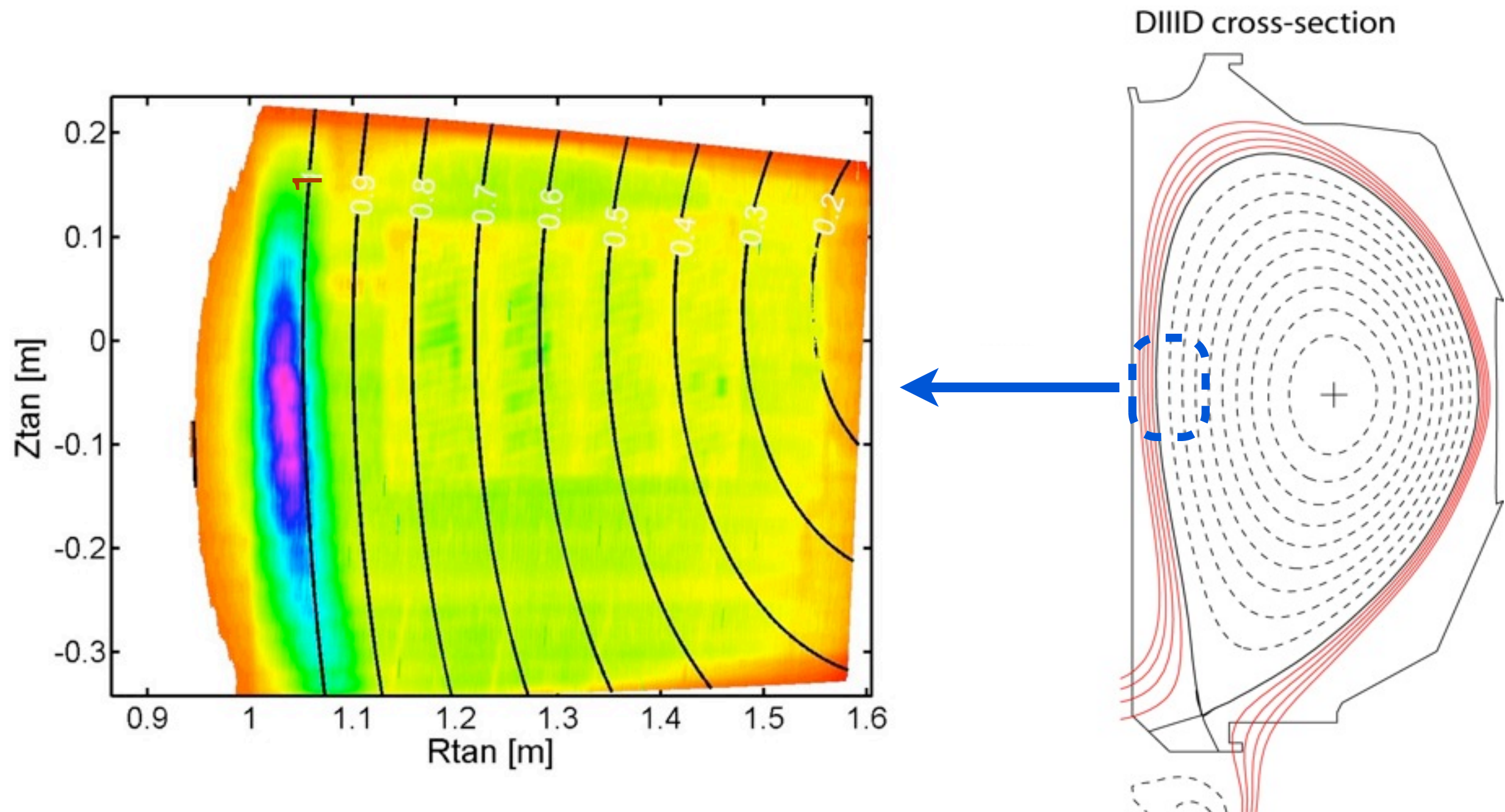
Calculated contrast



Choosing a waveplate with appropriate group delay to give sensitivity to high ion temperature

- Trade-off between group delay and contrast
- Larger wave delay improves velocity sensitivity

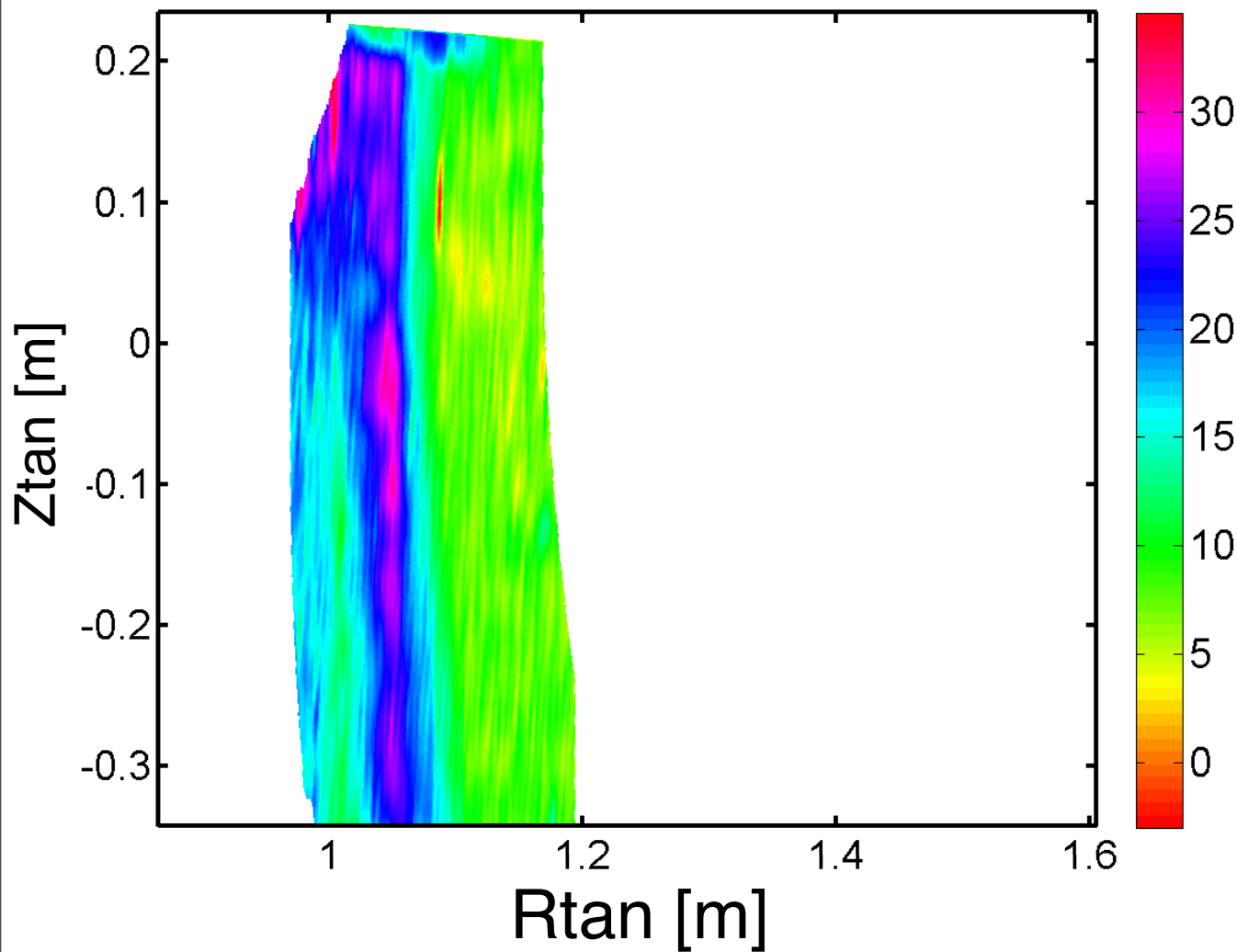
Measured CIII Brightness Profile is Localized at the Edge of the Plasma



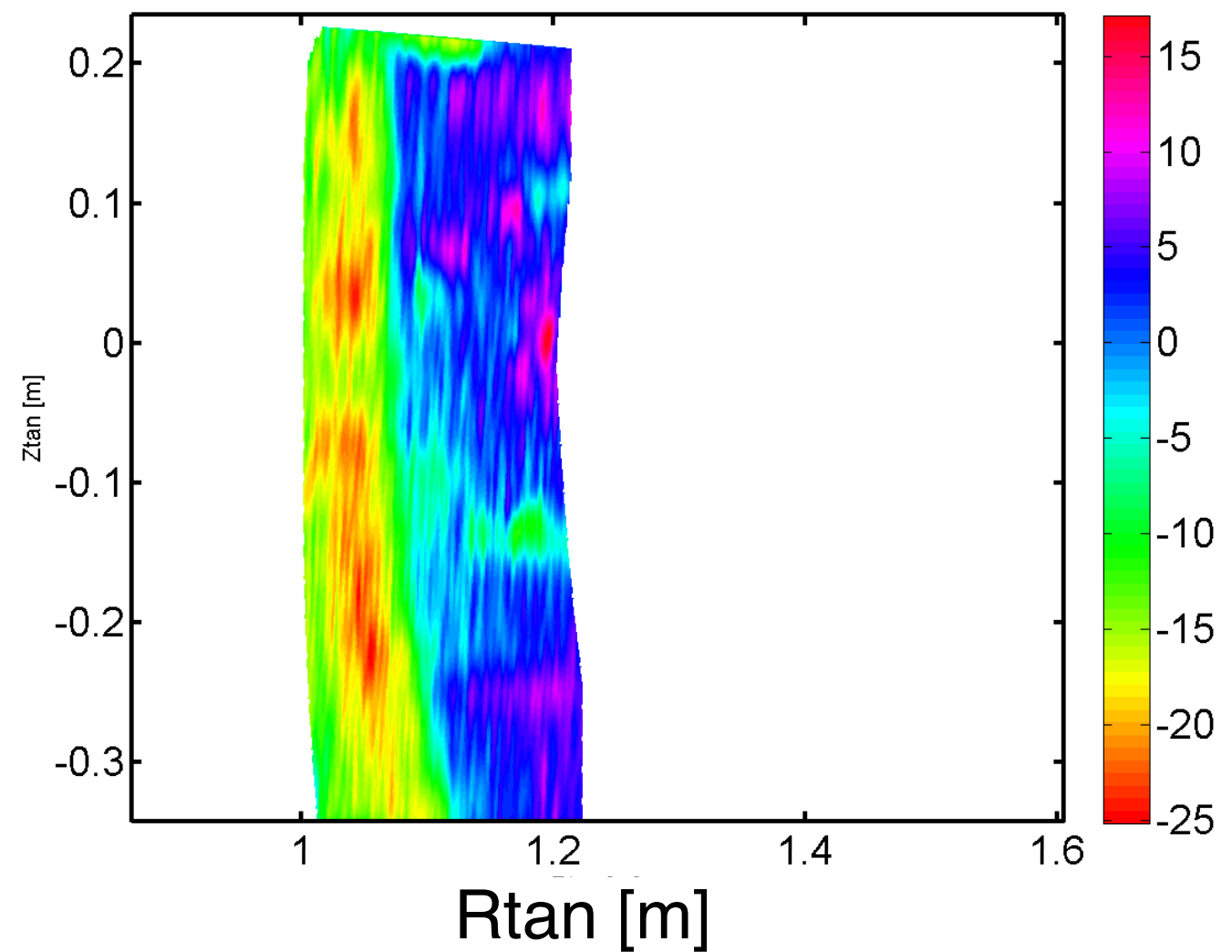
Phase Reversal Consistent with the Reversal of the Toroidal Current(I_p)

Phase Shift Images

Forward Current



Reverse Current

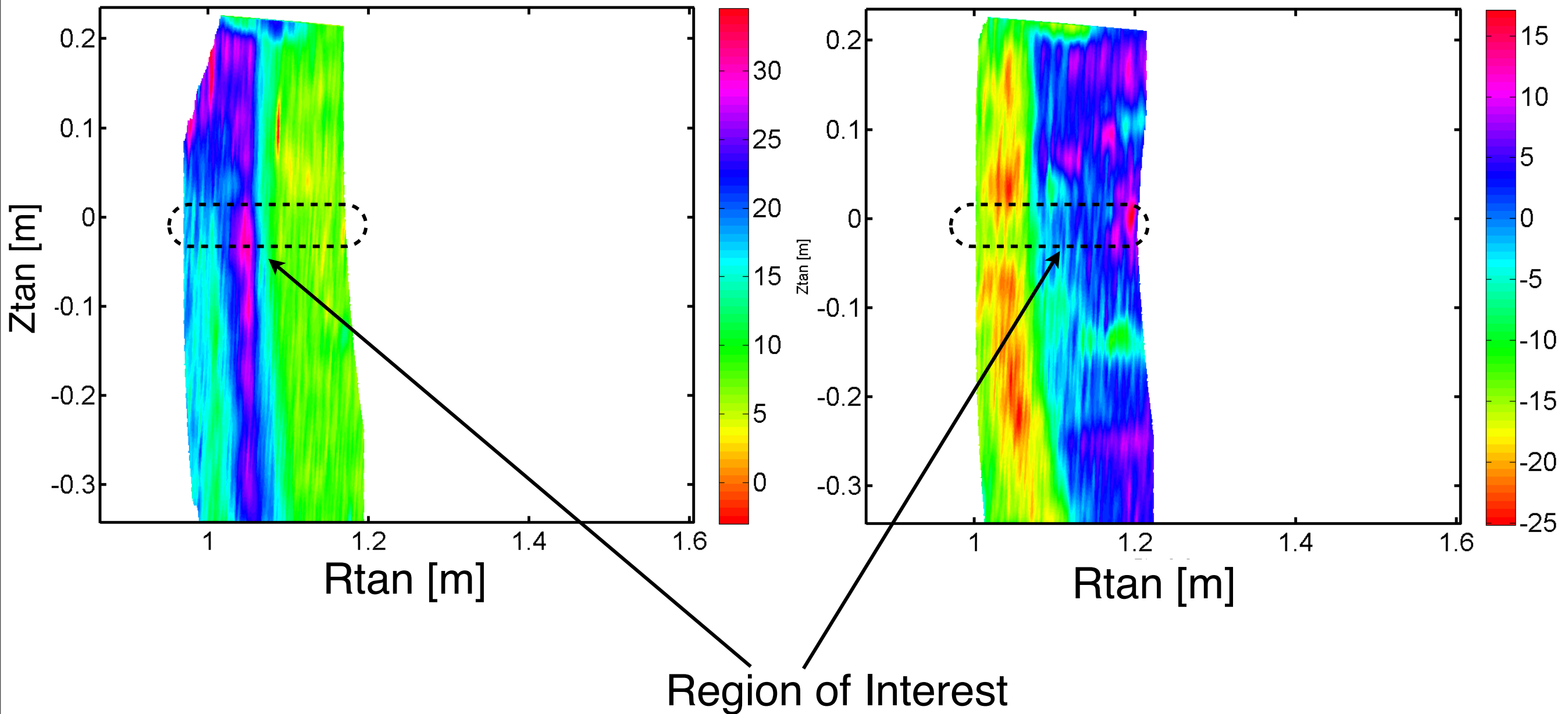


Phase Reversal Consistent with the Reversal of the Toroidal Current (I_p)

Phase Shift Images

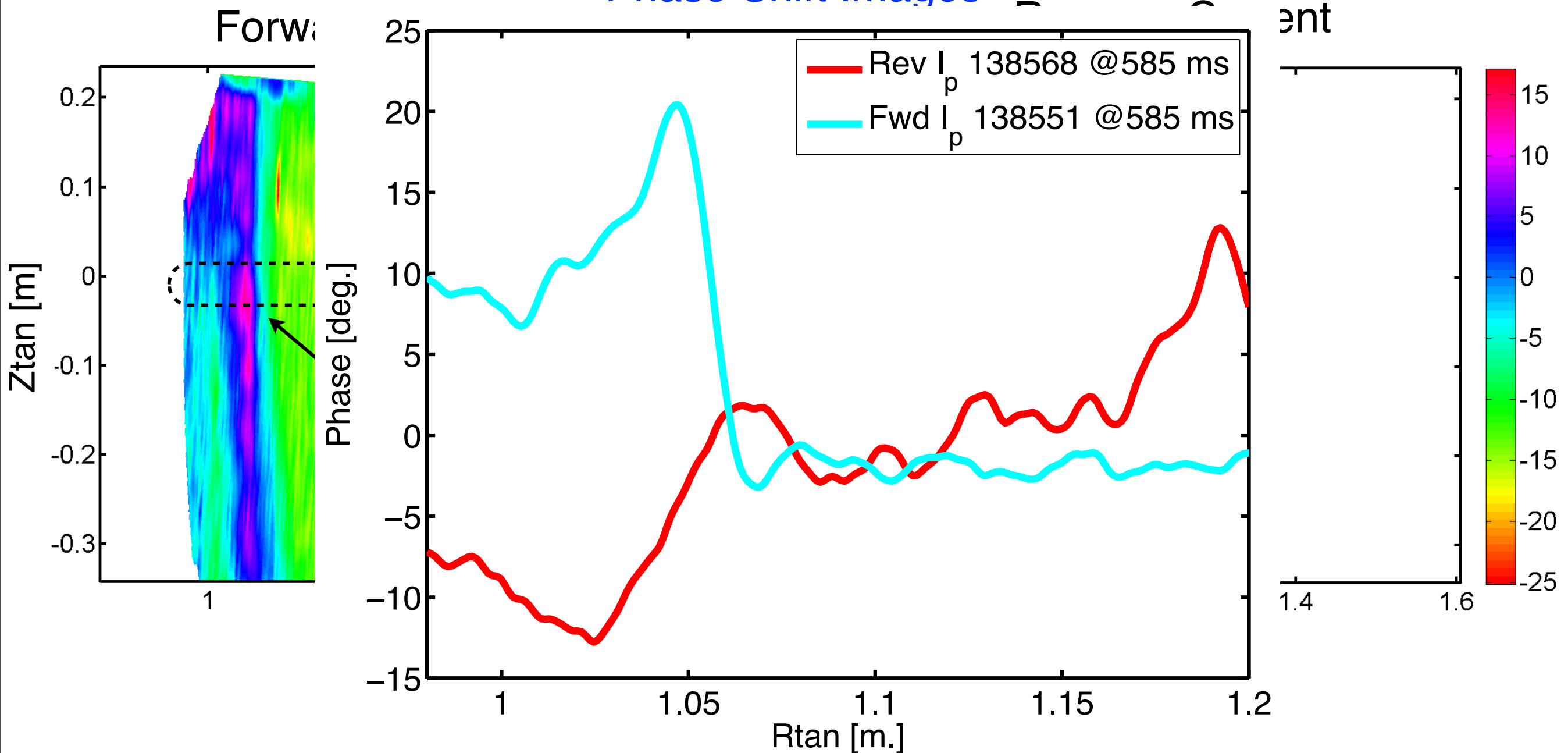
Forward Current

Reverse Current



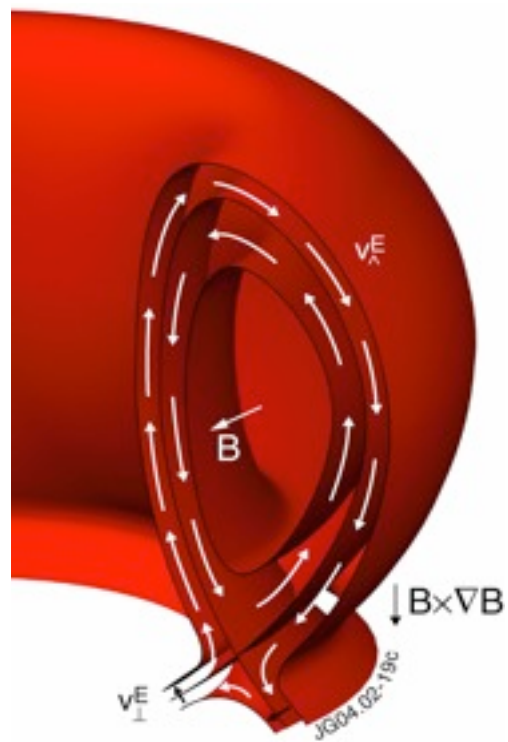
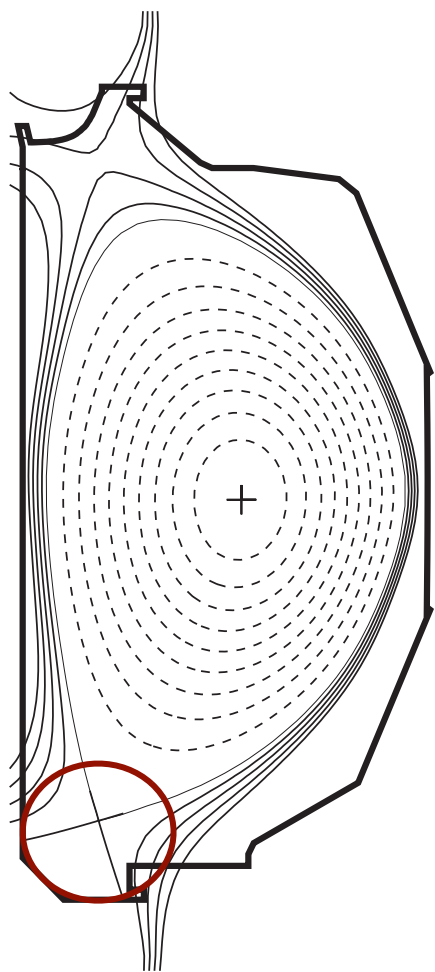
Phase Reversal Consistent with the Reversal of the Toroidal Current (I_p)

Phase Shift Images



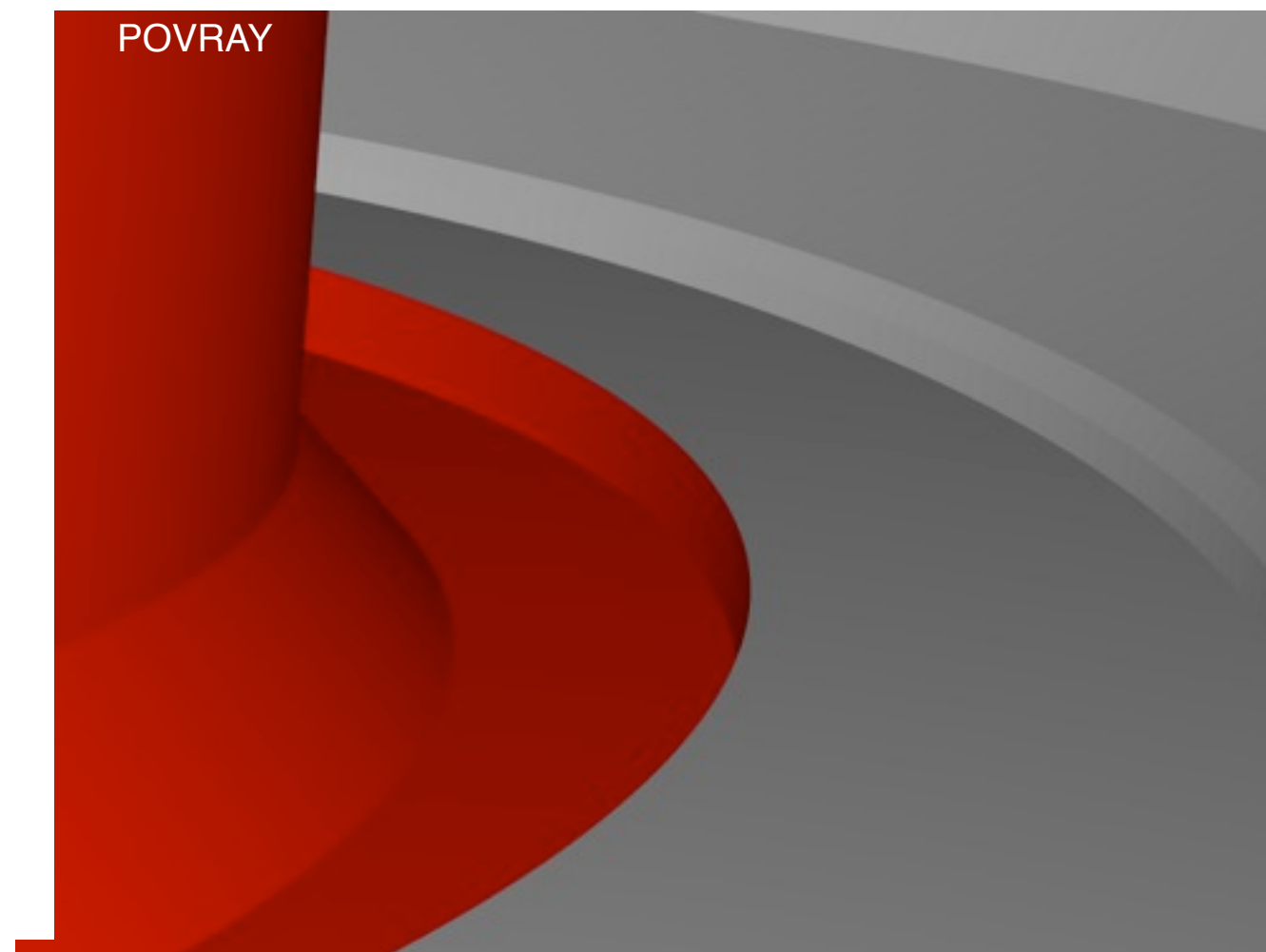
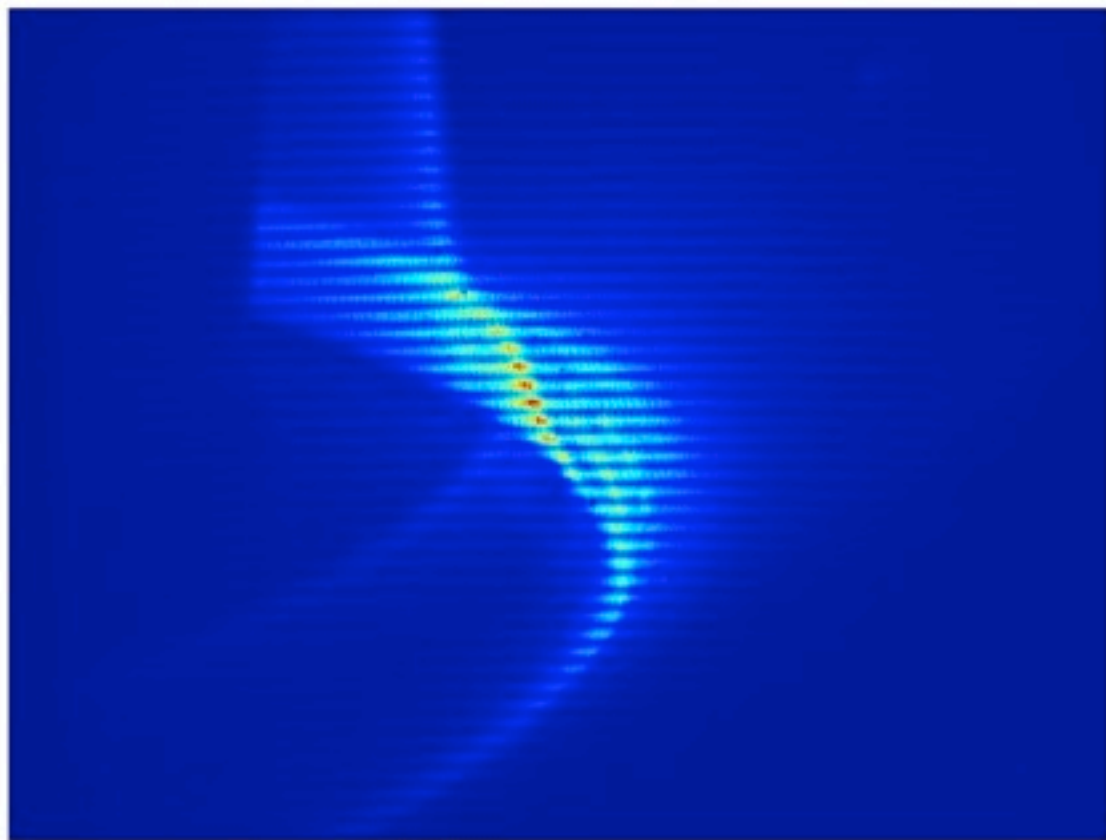
Reversal of flow agrees with other standard diagnostics

Divertor Flow Imaging Using CIII Emission



Divertor Flow Imaging Using CIII Emission

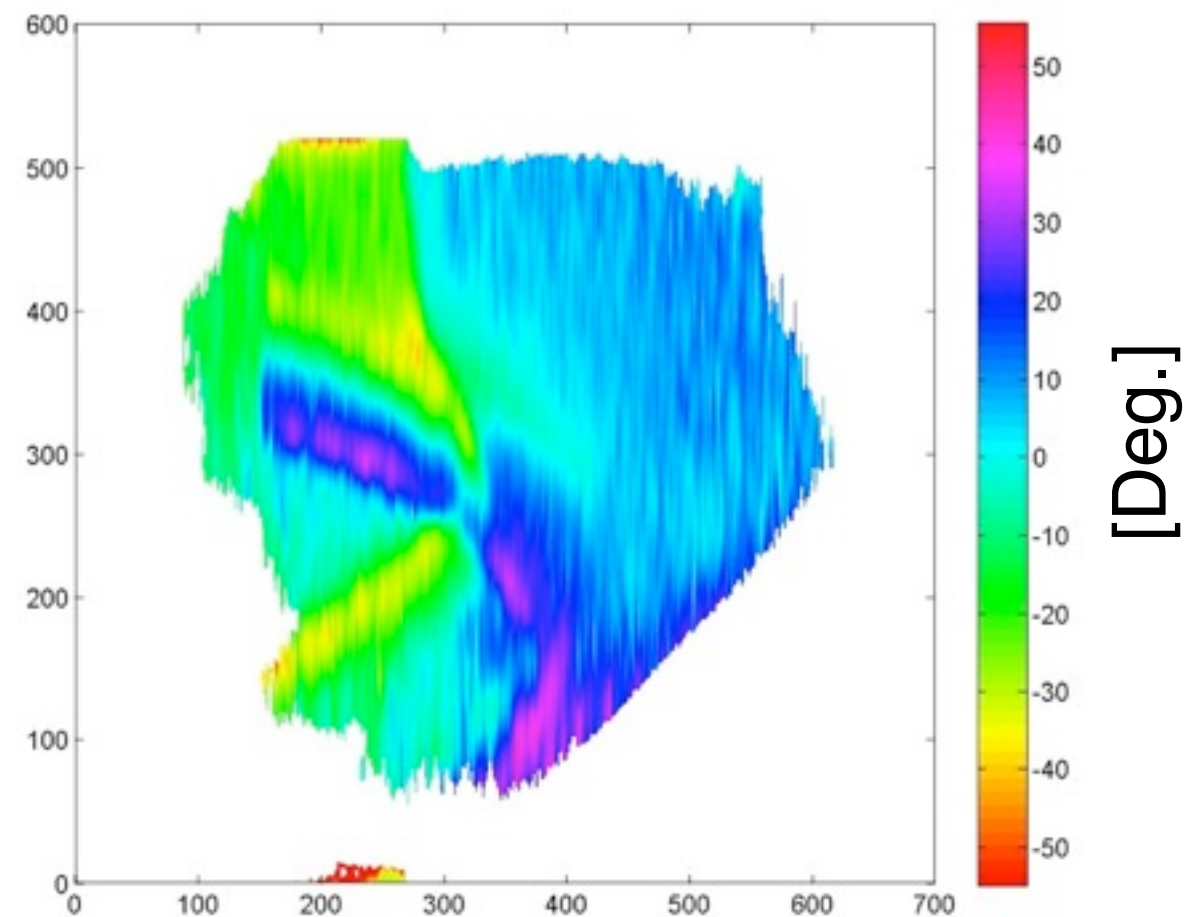
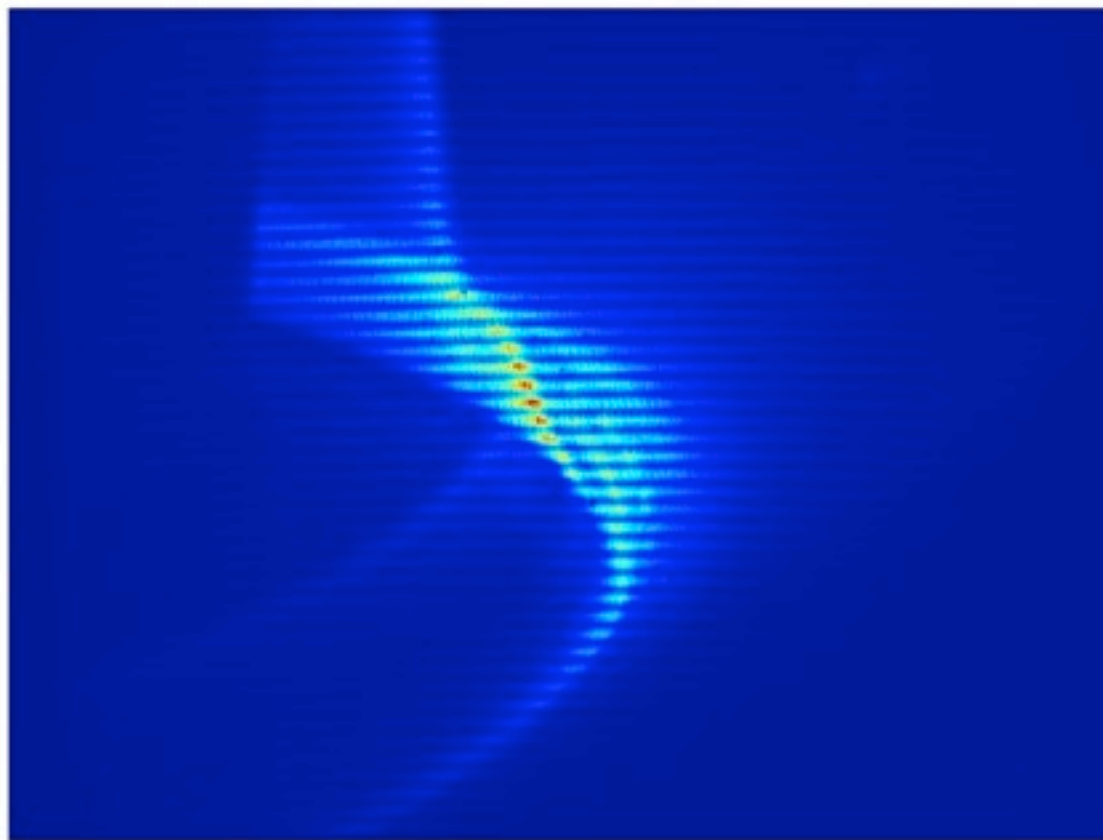
$$I = \frac{I_0}{2} [1 + \zeta \cos(\varphi_y + \varphi)]$$



Divertor Flow Imaging Using CIII Emission

$$I = \frac{I_0}{2} [1 + \zeta \cos(\varphi_y + \varphi)]$$

$$\vec{v} \cdot \hat{l} = \frac{\delta\varphi_{max}}{\kappa\varphi_0} c \sim 27 \text{ km.s}^{-1}$$



Complex flow pattern structure requires a 3D unfolding!

Movie Showing the Time Evolution of Divertor Flow Pattern

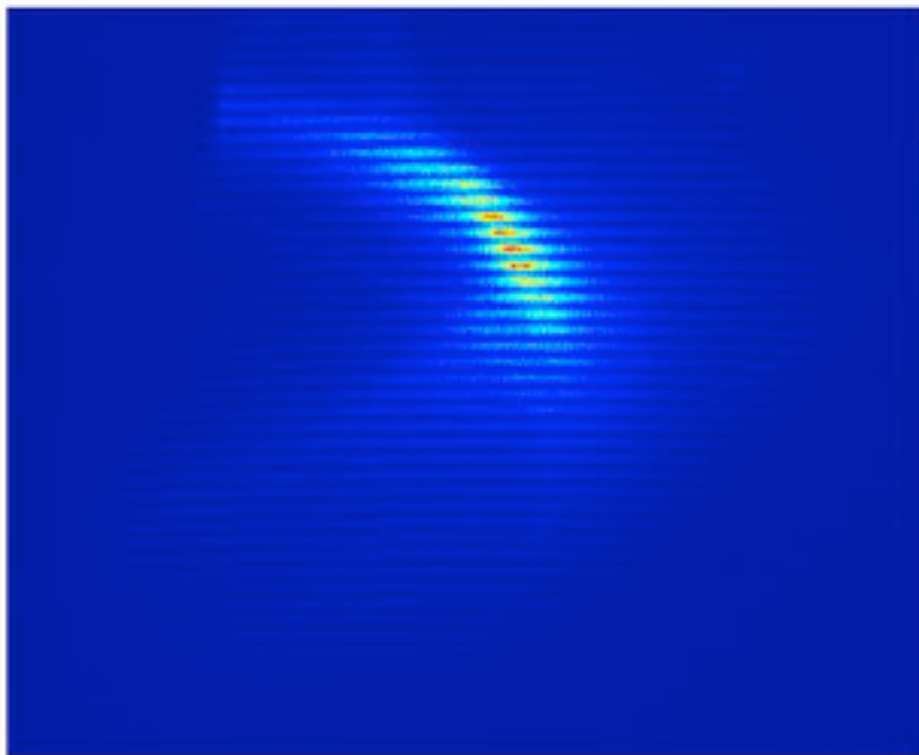
Raw Image

Demodulated Image: Phase shift

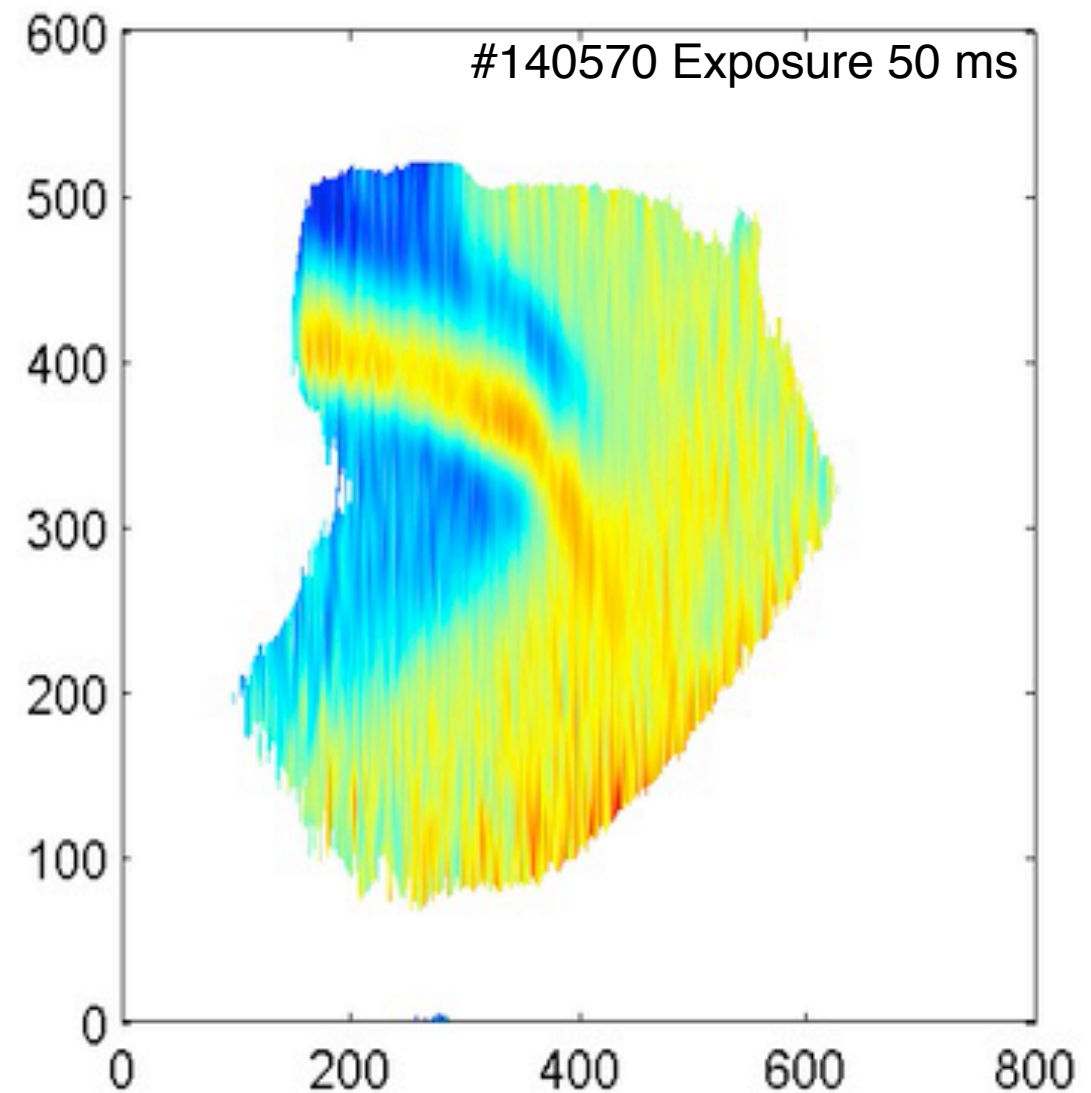
#140570 Exposure 50 ms

Movie Showing the Time Evolution of Divertor Flow Pattern

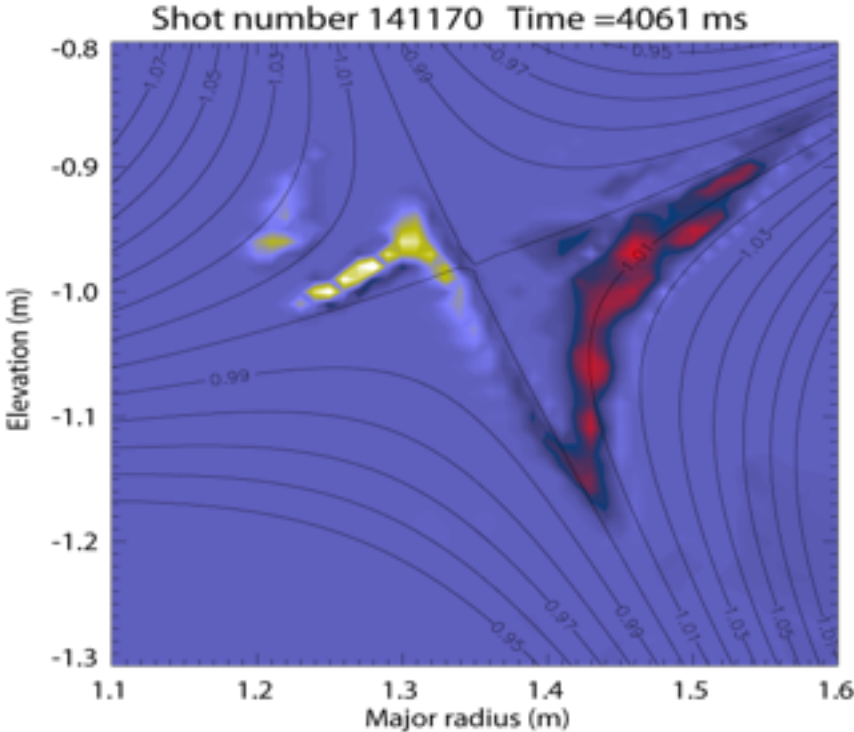
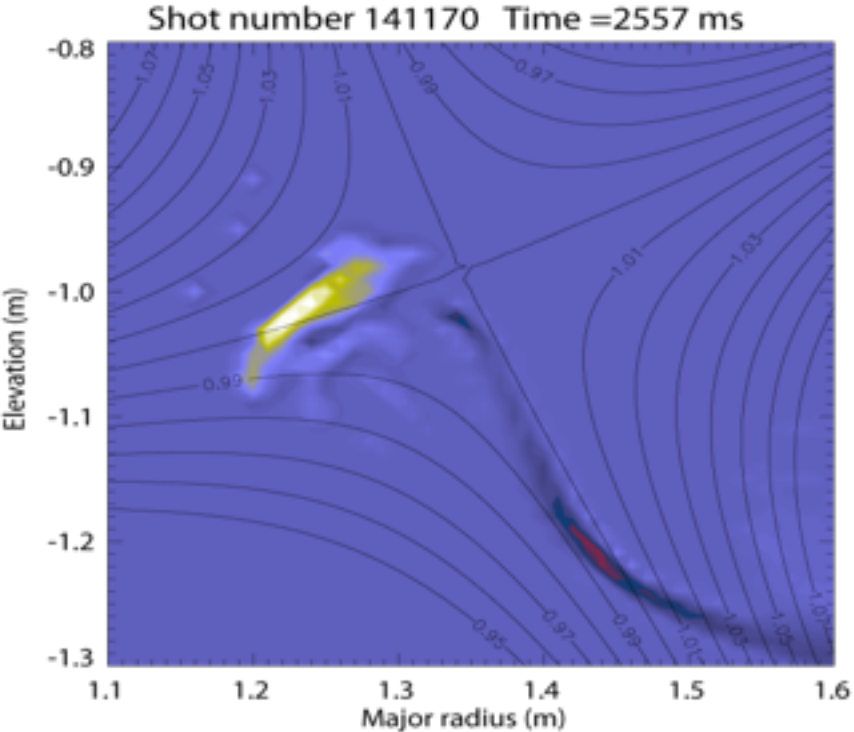
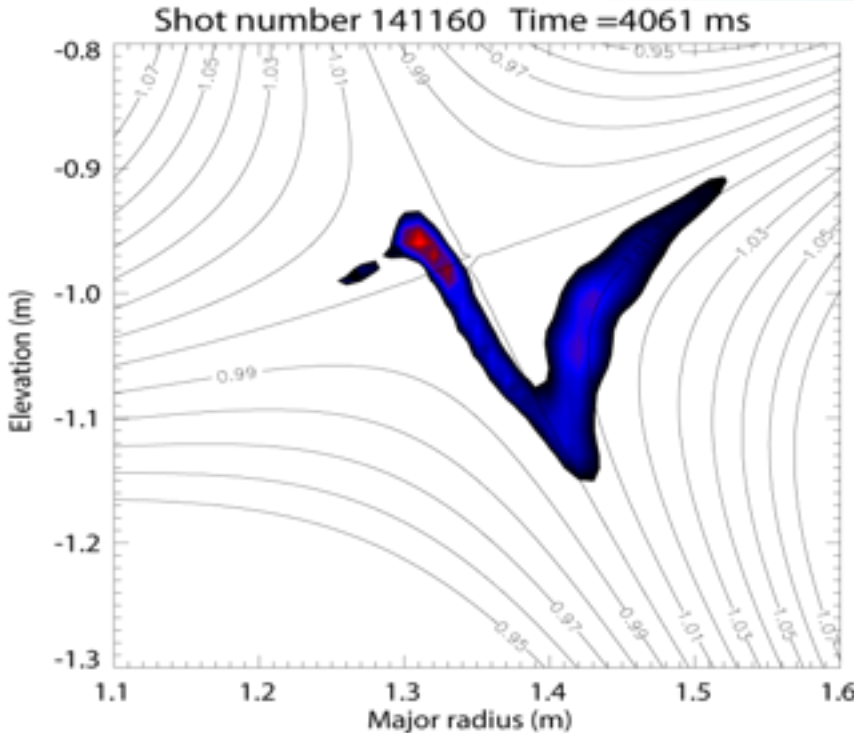
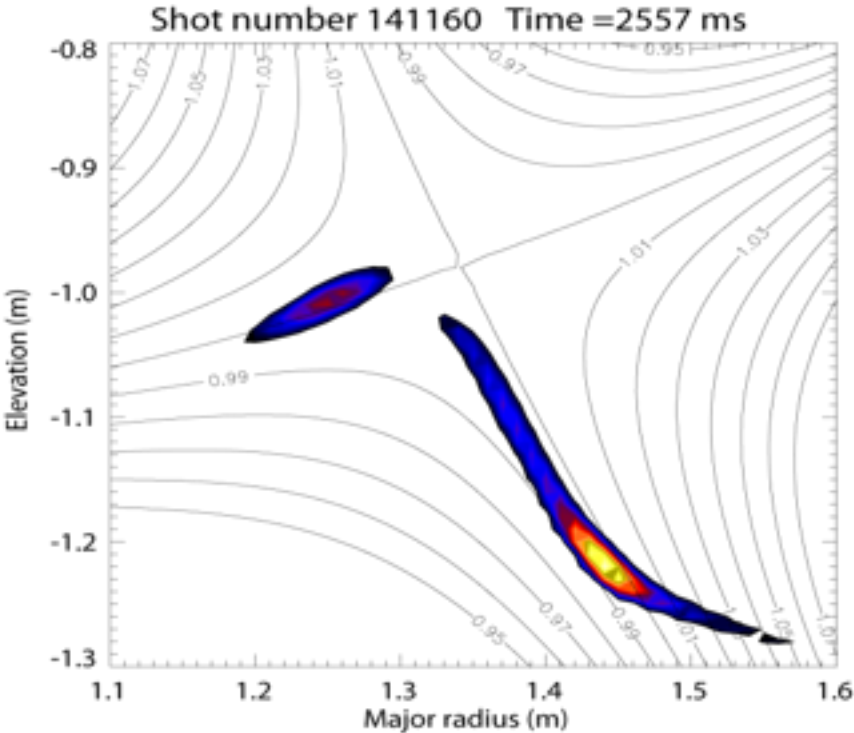
Raw Image



Demodulated Image: Phase shift



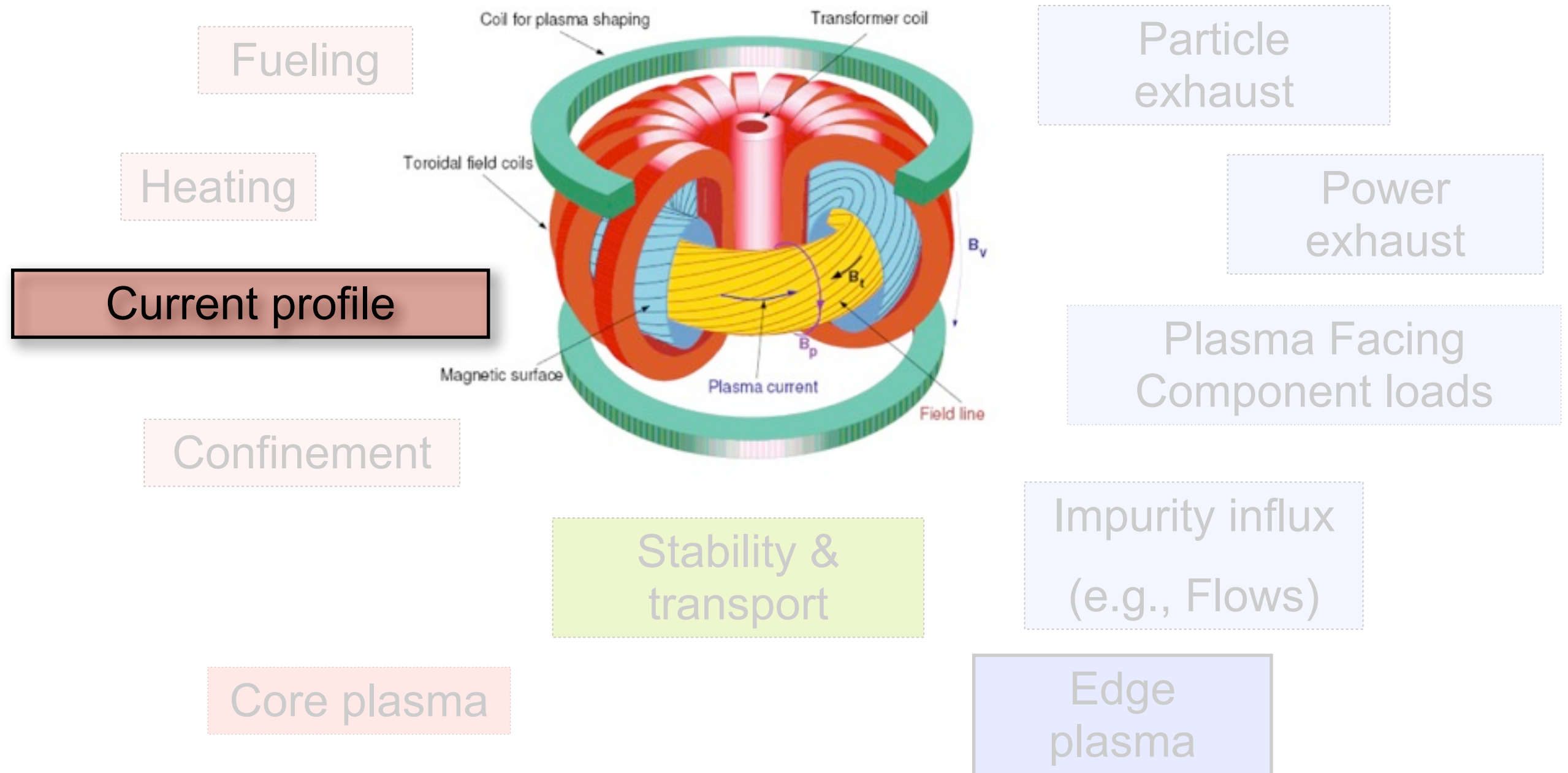
Reconstructed Brightness and Flow Profiles Conform with Equilibrium Surfaces



Short Summary/Outlook

- First 2D flow pattern imaging using a polarization interferometer
- Preliminary results show evidence of flow reversal with plasma current consistent with standard diagnostics
- Divertor imaging show complex flow structure of great interest for modelers
- Comparison with array of edge modeling codes
- Target multiple species for wider spatial coverage on NSTX
- Extension to Laser Induced Fluorescence- and Gas Puffing- assisted flow measurements are under investigation.

Key Components of Plasmas Generated in a Tokamak



Motional Stark Effect enables Measurements of the Magnetic Field Pitch Angle

Injected beam atoms feel induced electric field in frame of the beam

Doppler shift from thermal H_α

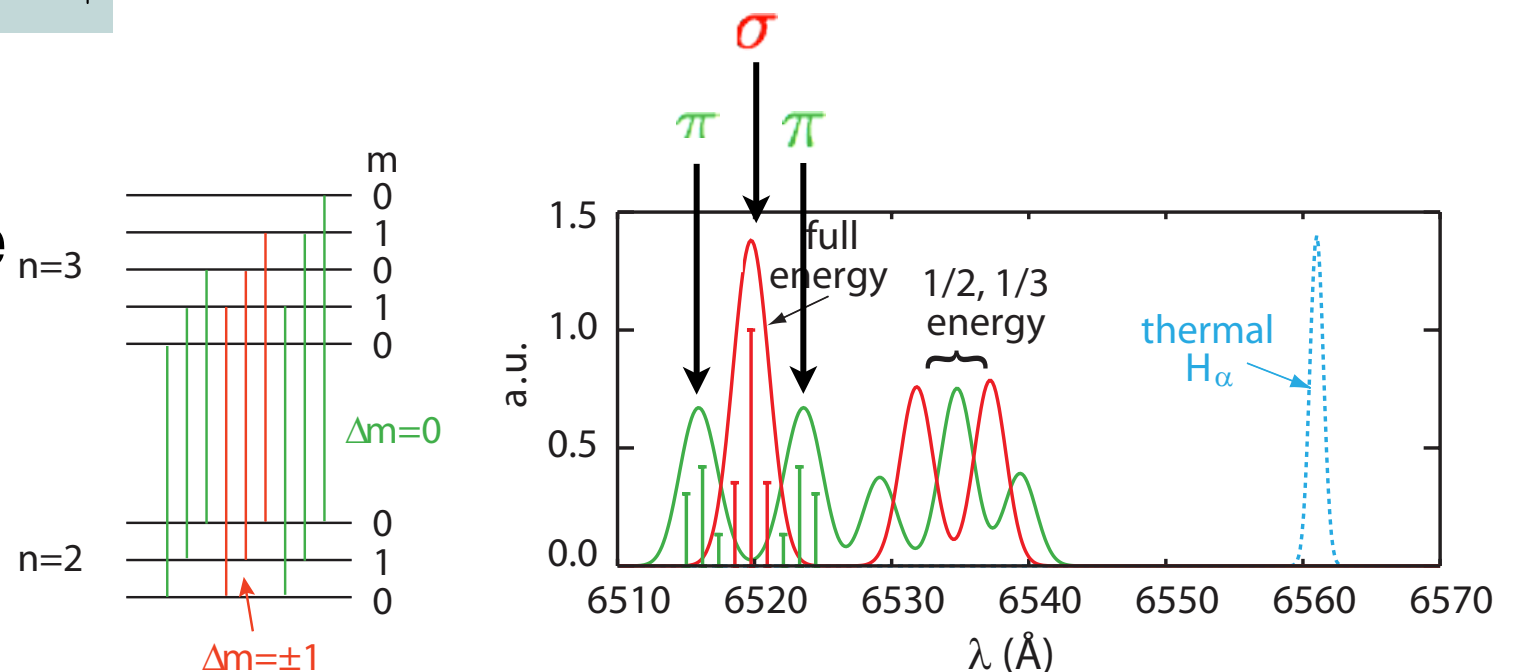
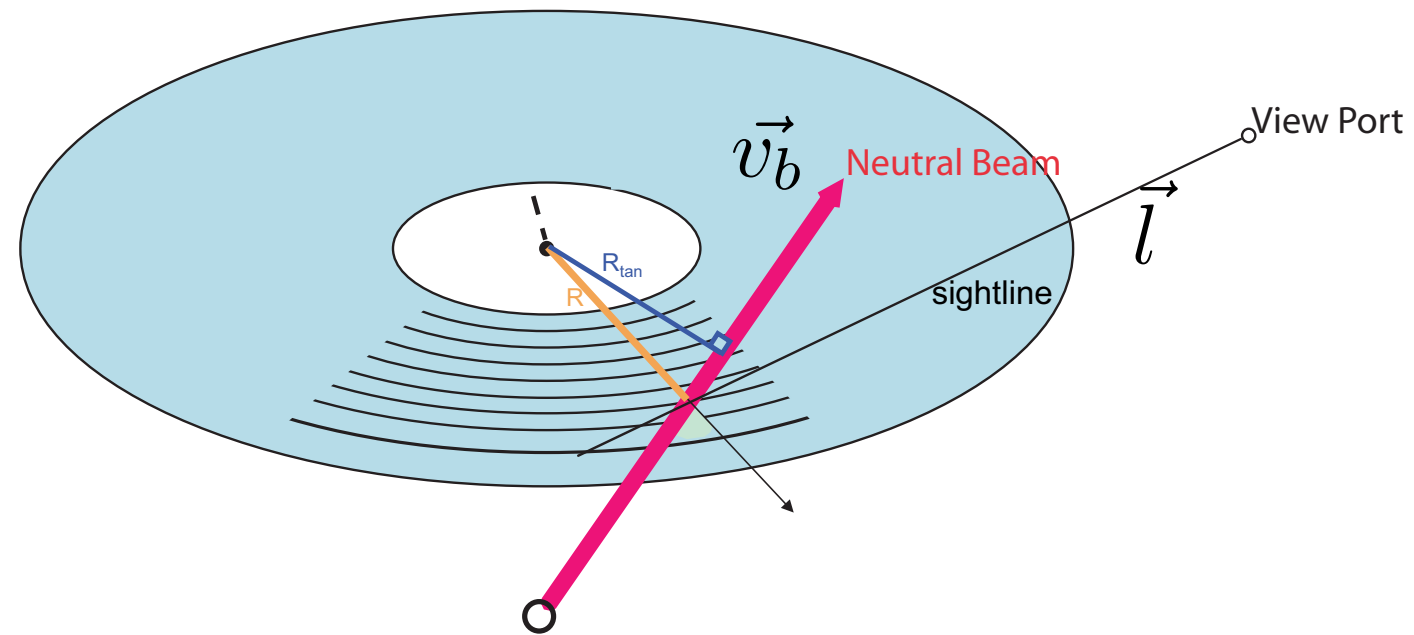
$$\delta\lambda = \lambda_\alpha \frac{\hat{v}_b \cdot \hat{l}}{c}$$

Split by Stark effect

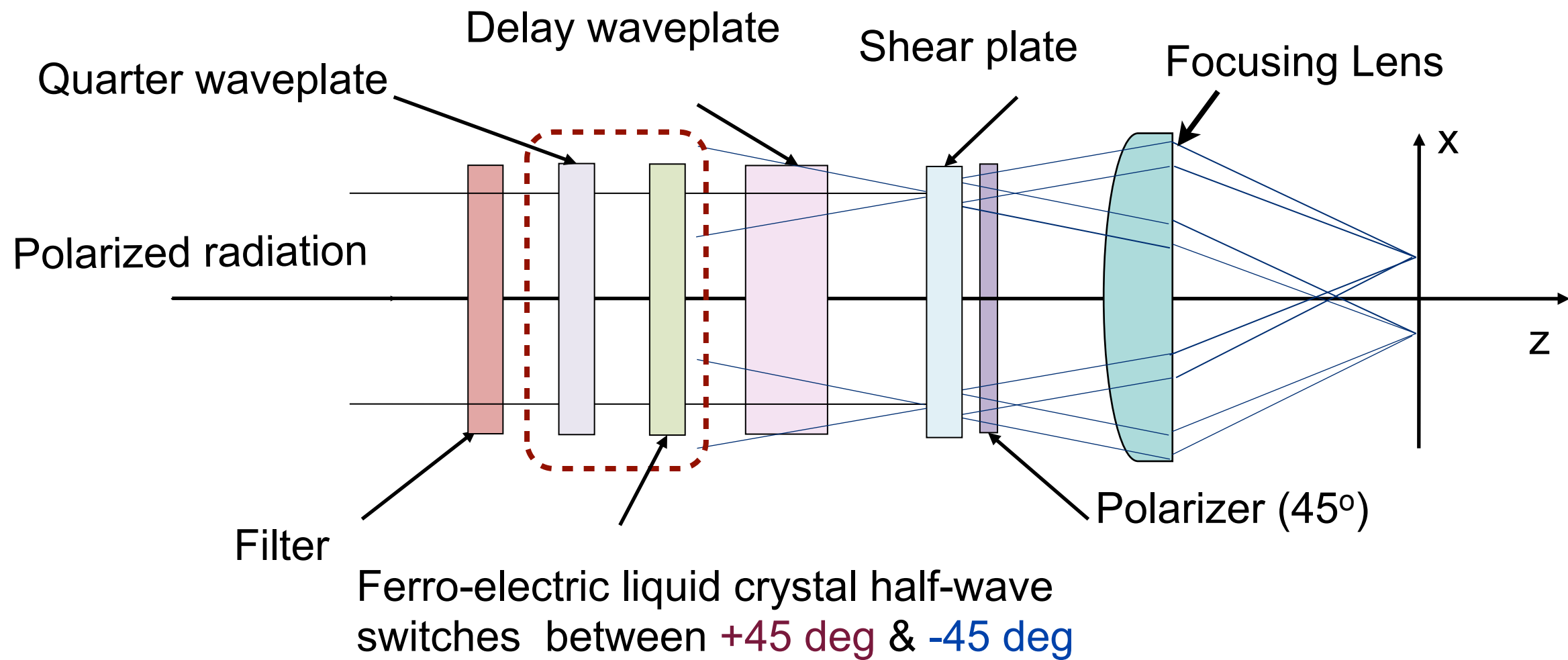
$$\Delta\lambda_s = 2.7574 \times 10^{-8} E \text{ [nm]} \text{ where } E = |\vec{v}_b \times \vec{B}|$$

$$\vec{B} = \vec{B}_\varphi + \vec{B}_\theta$$

Measuring the polarization of the multiplet yields the orientation of the internal magnetic field



Shearing Polarization Interferometer Used to Encode Information of the Stark Multiplet



$$S = I[1 + \zeta \cos(k_y y + \varphi + 2\theta)]$$

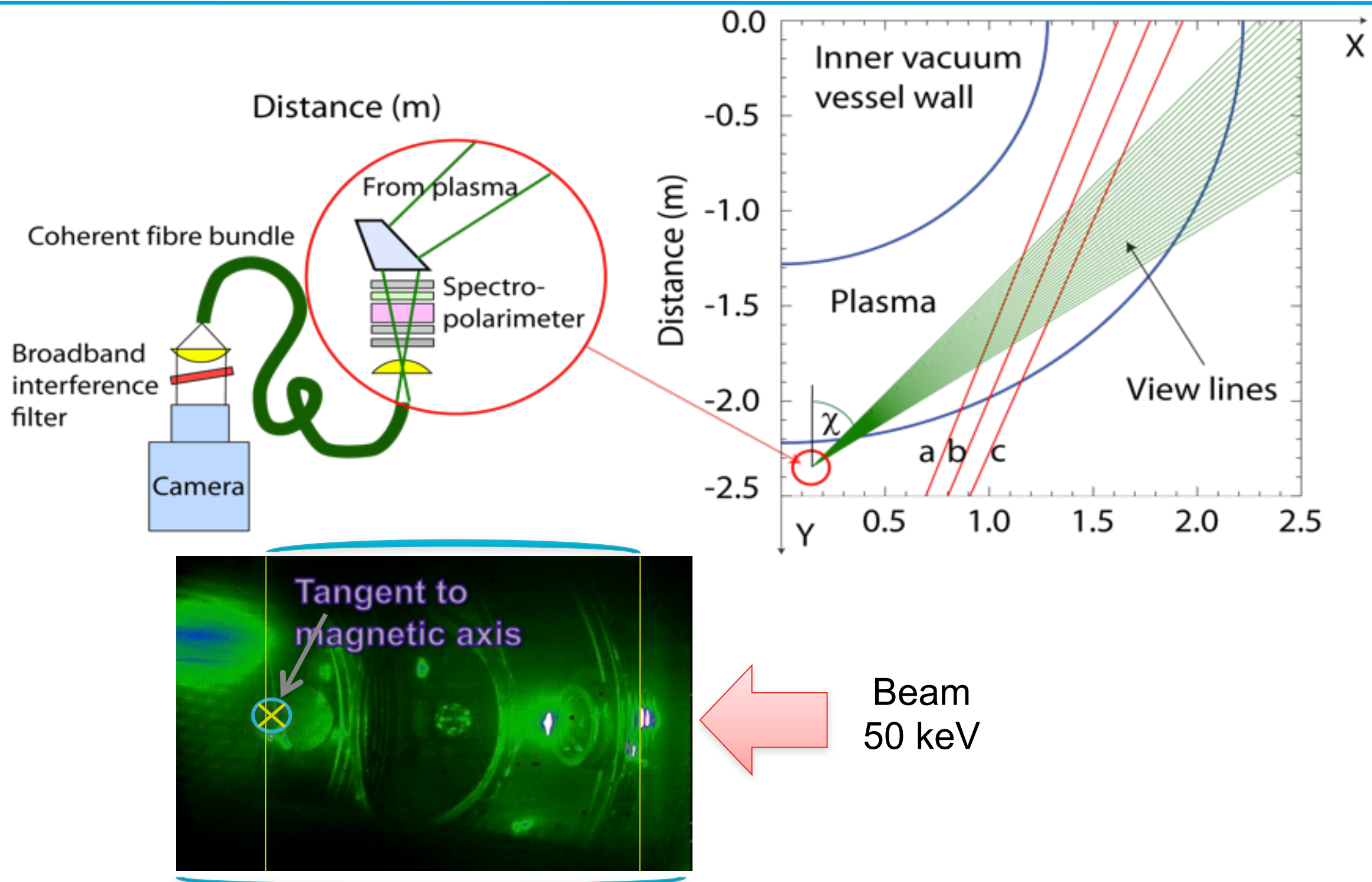
$$S = I[1 + \zeta \cos(k_y y + \varphi - 2\theta)]$$

Image pair yields 4x the polarization angle

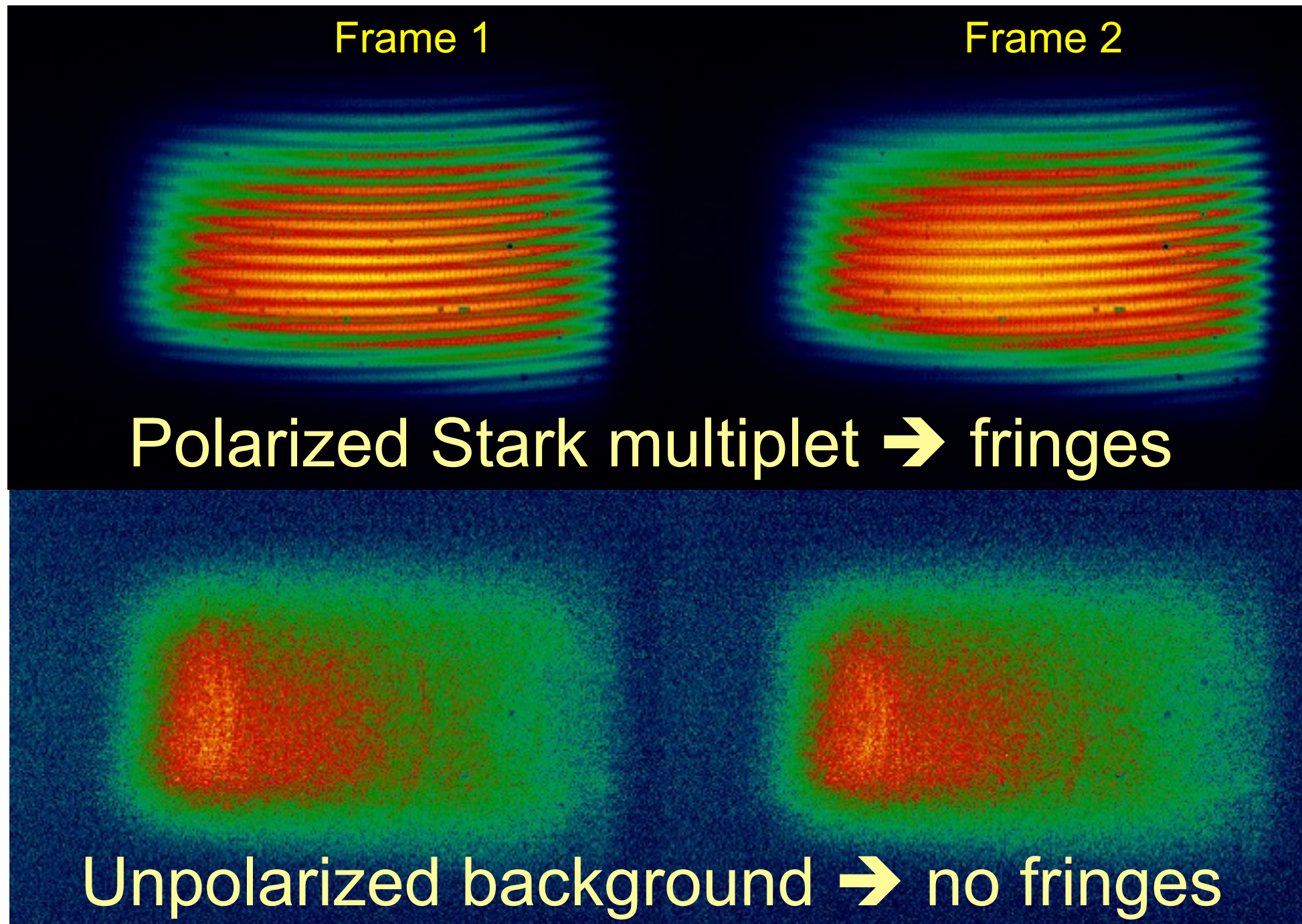
Outline

- How to image flows and the current profile?
 - Polarization interferometer
 - Spatial heterodyne system
- **Applications**
 - Imaging of Doppler flows (DIIID)
 - **Magnetic field pitch angle map (TEXTOR)**
- Summary and Outlook

Applications to Measuring the Magnetic Pitch Angle: TEXTOR Viewing Geometry



Polarized Emission Generates Interference Fringes



Beam on

Beam off

Interference Pattern: Beam Footprint Interferogram

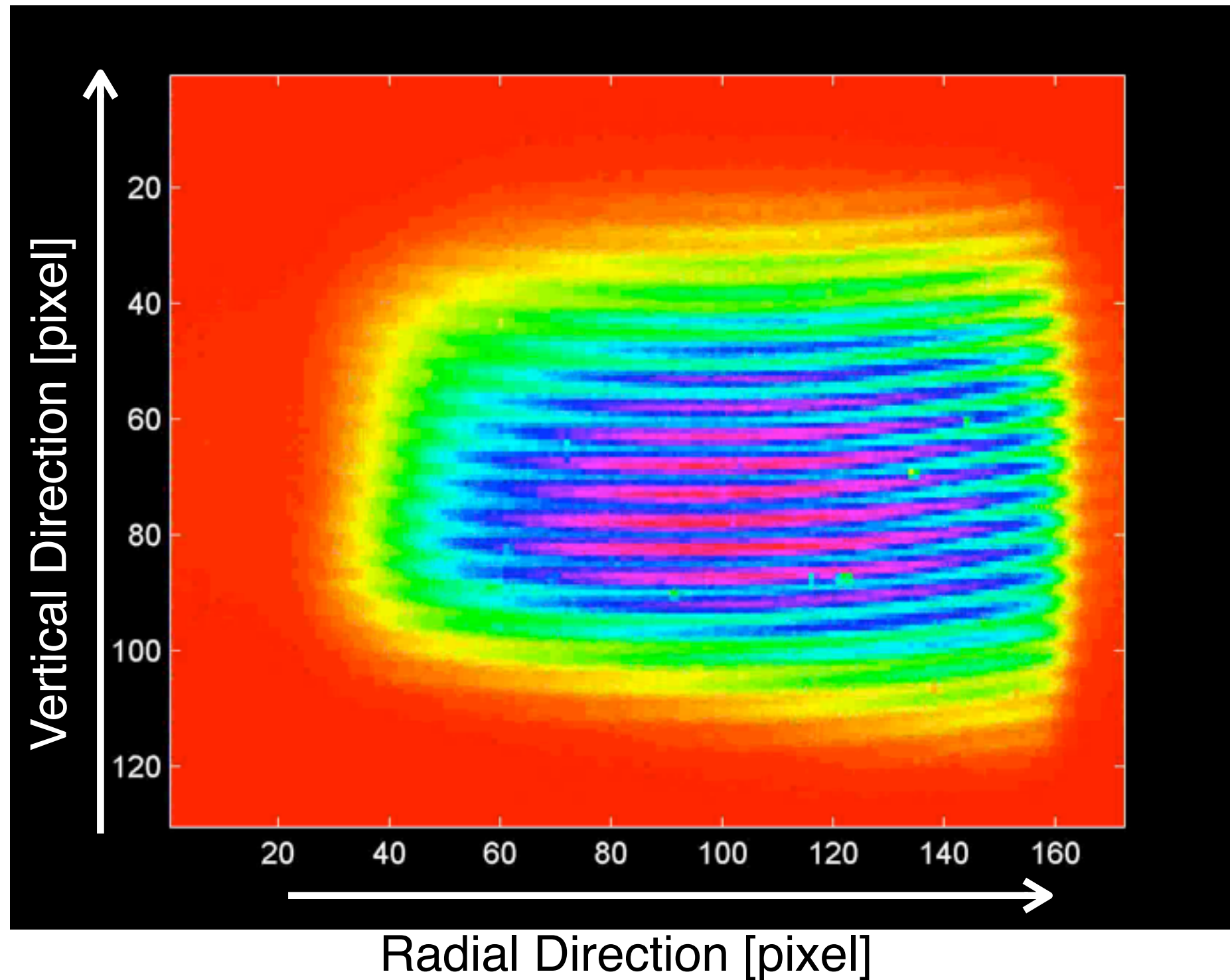
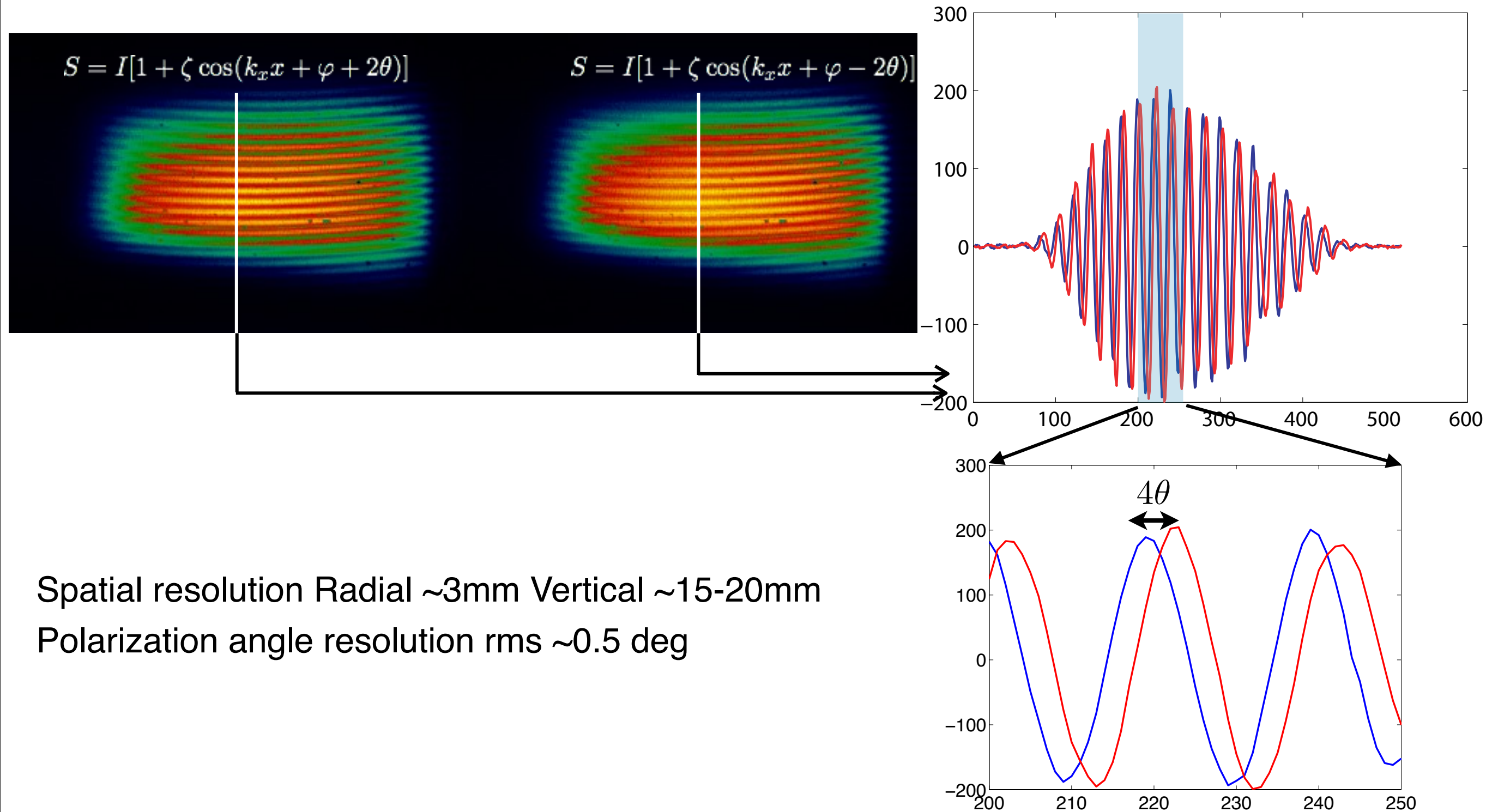


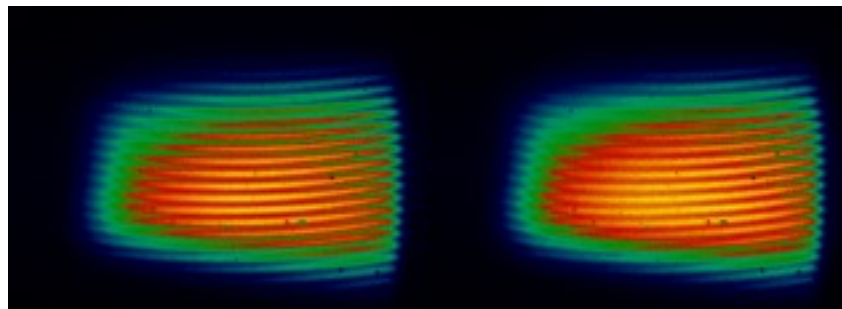
Image pair phase difference yields 4x polarization angle: Results



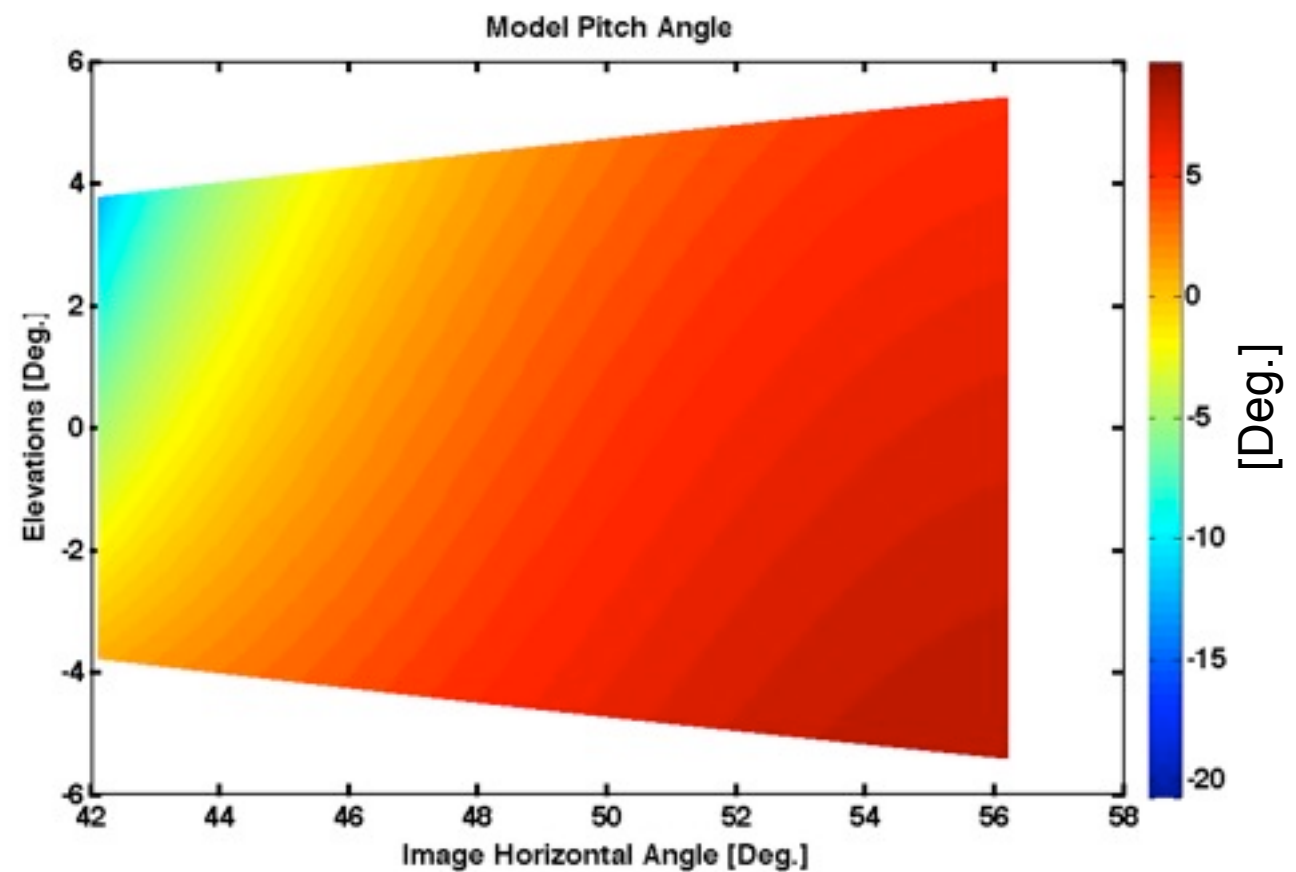
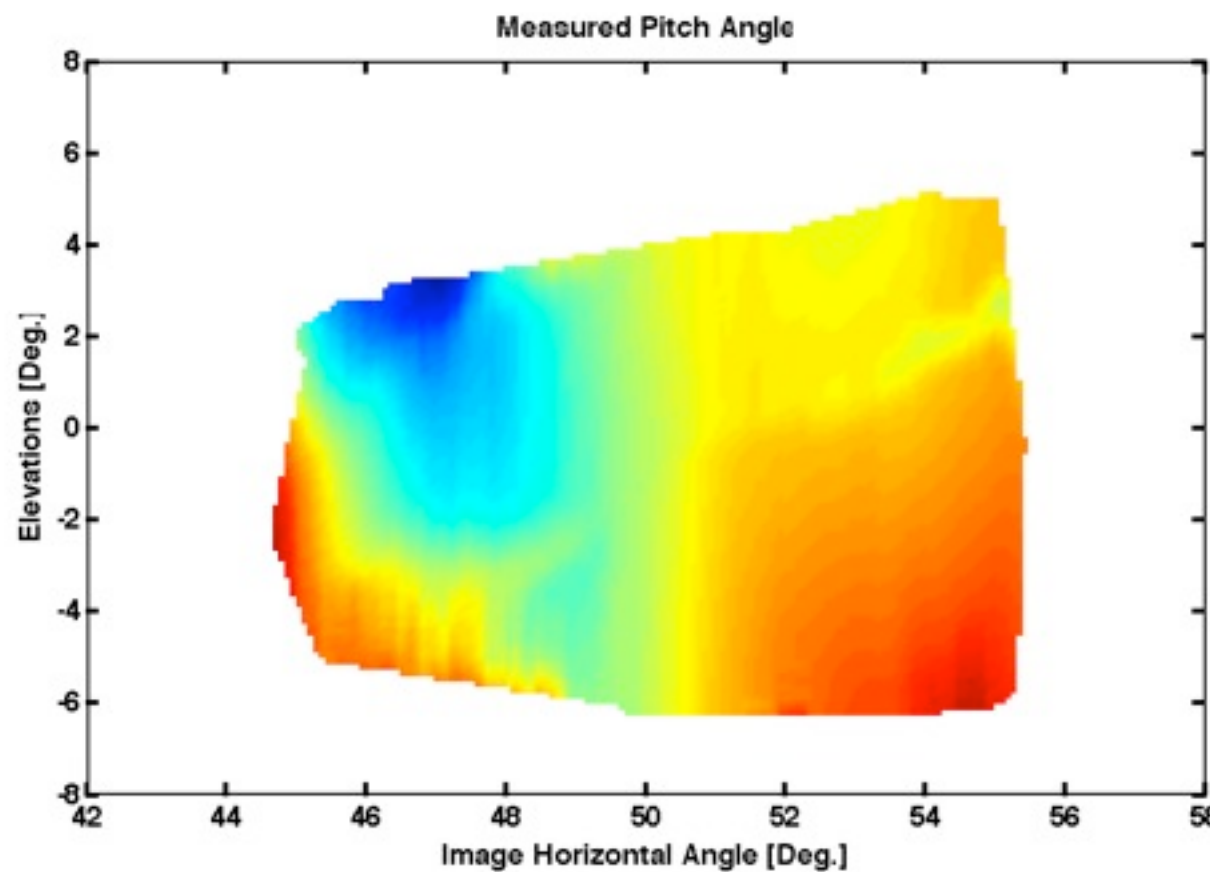
Spatial resolution Radial $\sim 3\text{mm}$ Vertical $\sim 15\text{-}20\text{mm}$

Polarization angle resolution rms ~ 0.5 deg

2D Field Pitch Angle Map: Experiment and Simple Model

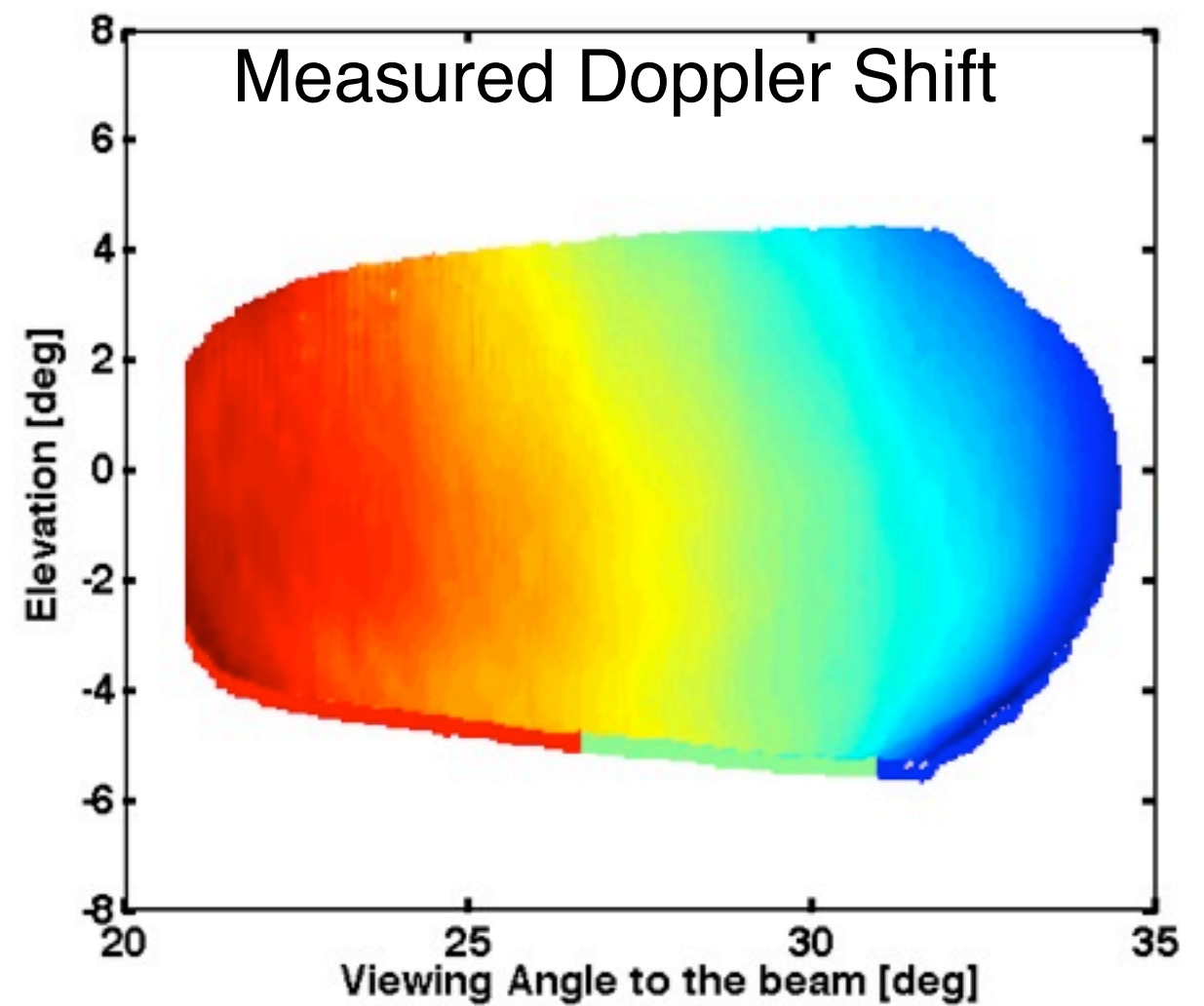
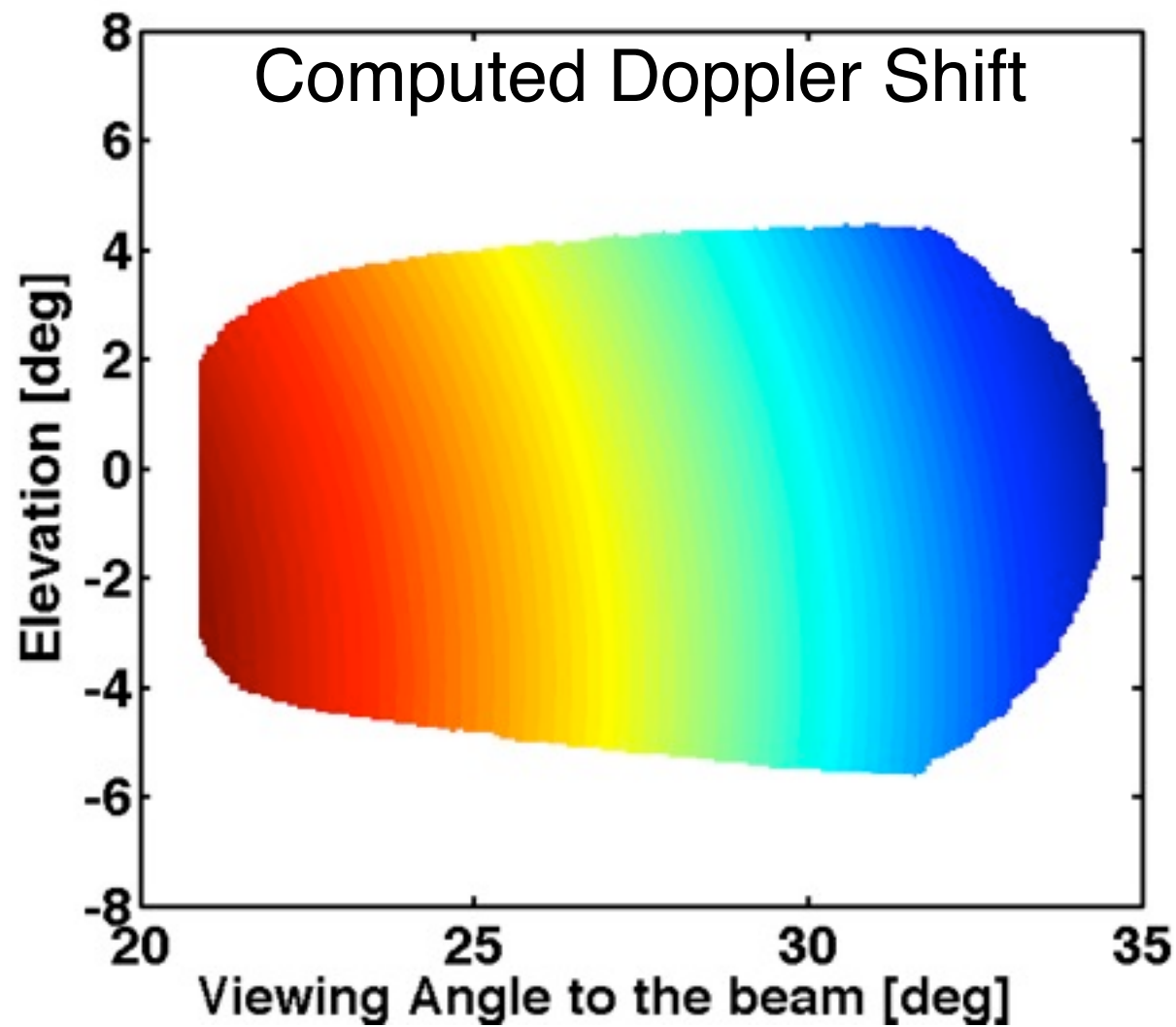


Spatial resolution Radial $\sim 3\text{mm}$ Vertical $\sim 15\text{-}20\text{mm}$
Polarization angle resolution rms ~ 0.5 deg



Discrepancies are due to imperfections of coupling prism

Beam Doppler Phase Shift: Experiment vs Model



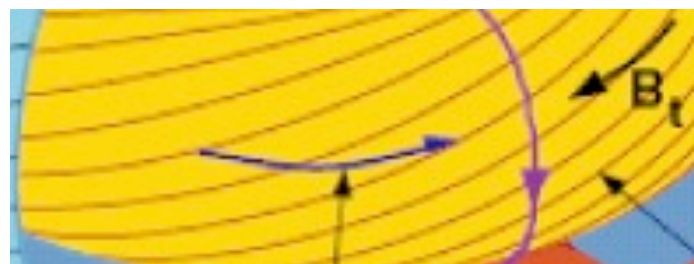
Agreement between Doppler shift and model

Summary and Next Steps

- ✓ Imaging provides a clear advantage over standard single point measurements
- ✓ First 2D pitch angle map agrees with a simple model
- * Next step: Applications of this imaging technique to resolve coherent events
- * More work is required to obtain the flux function from the pitch map

Backup Slides

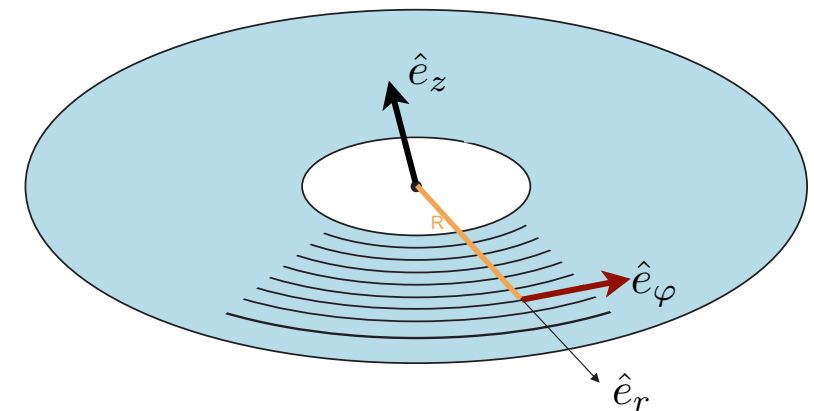
Direct Measurement of the Flux Function



Plasma Current

Helical field line

Top view



$$\tan \beta = \frac{A_1 B_z + A_2 B_r + A_3 B_\varphi}{A_4 B_z + A_5 B_r + A_6 B_\varphi} \text{ where } A_k \text{ are geometric factors.}$$

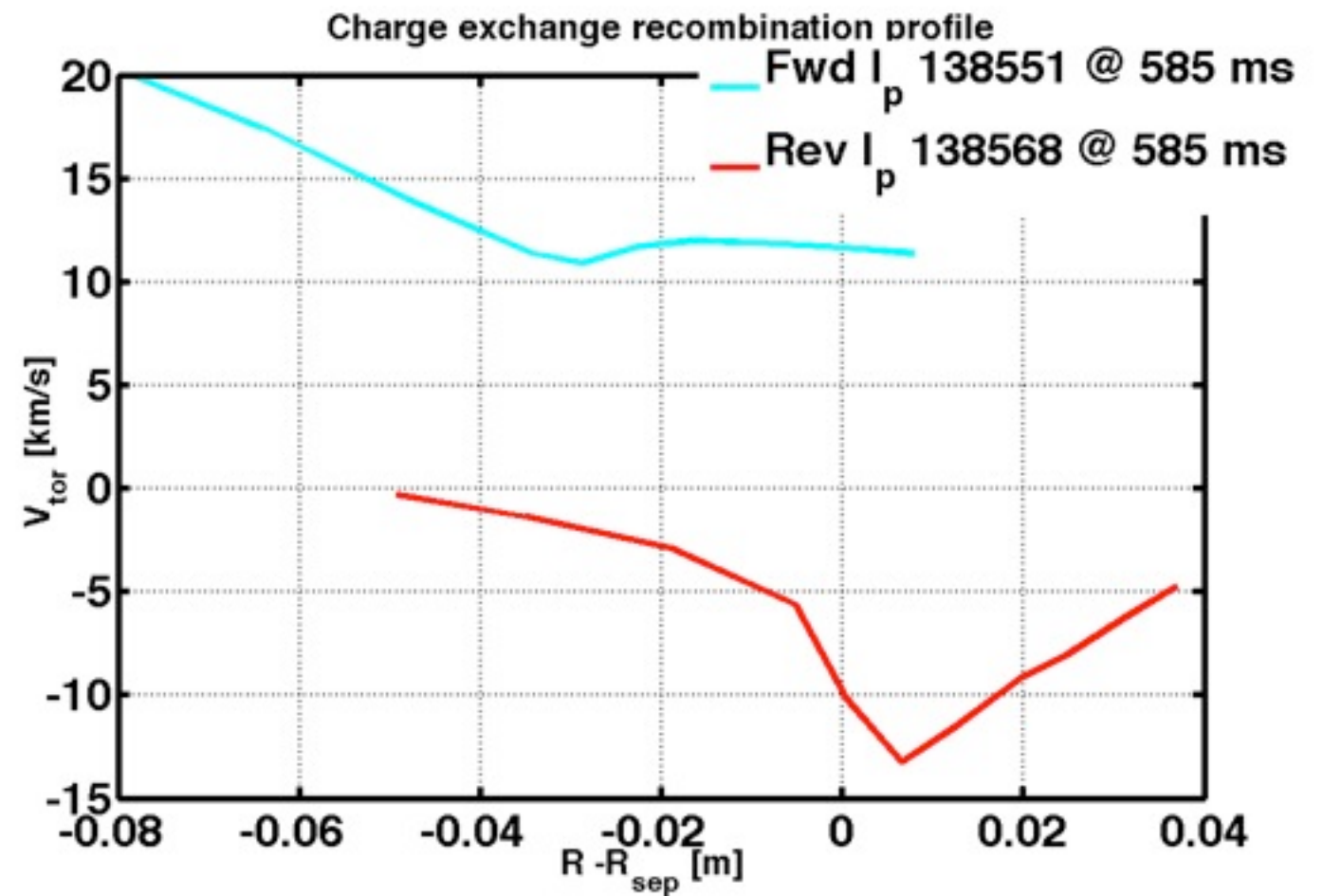
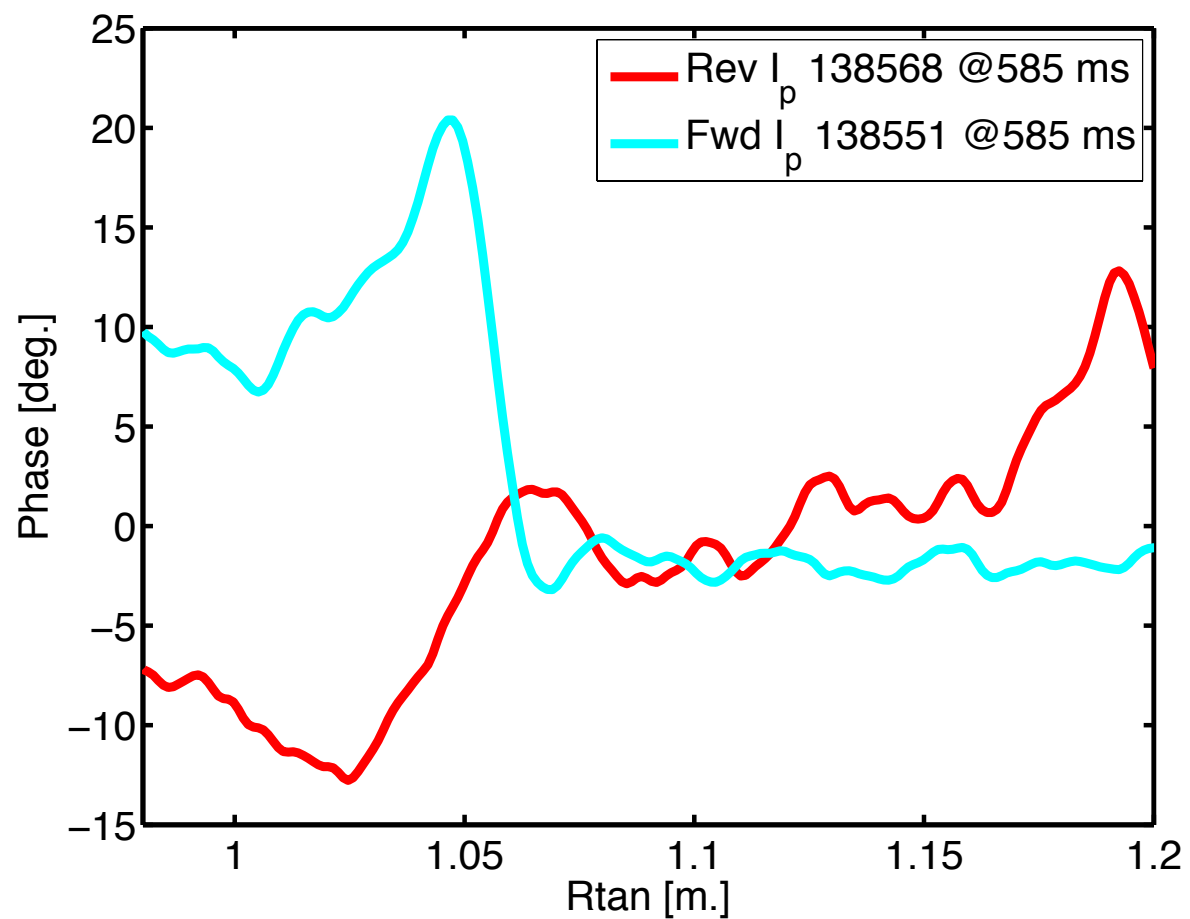
Rewrite $S = B_z + \alpha Br$; Recall $\nabla \times B = \mu_0 J$

$$B_r = \frac{1}{r} \frac{\partial \psi}{\partial z} \text{ and } B_z = -\frac{1}{r} \frac{\partial \psi}{\partial r} \Rightarrow rS = \frac{\partial \psi}{\partial r} - \alpha \frac{\partial \psi}{\partial z}$$

$$\text{Let } u = r - z/\alpha, \quad rS = \frac{\partial \psi}{\partial u} \Rightarrow \int rS du = \psi(u_2) - \psi(u_1)$$

2D pitch angle mapping enables the reconstruction of the magnetic flux function and the current profile.

Comparison with Charge Exchange Recombination Profile (CVI)



Sign reversal is consistent with standard measurements

Implementation of Doppler Imaging Instrument

$$I = \frac{I_0}{2} [1 + \zeta \cos(\varphi_y) + \varphi]$$

$$\varphi = \frac{2\pi B(\lambda)L}{\lambda} \Rightarrow \varphi = \varphi_0 \left(1 + \kappa \frac{\vec{v} \cdot \hat{l}}{c}\right) \quad \kappa = \frac{\lambda}{B} \frac{\partial B}{\partial \lambda} \Big|_{\lambda_0}$$

